3-2014

Towards a Better Treatment of Parkinson's disease

Bradley Darryl Karain
Loma Linda University

LOMA LINDA UNIVERSITY
School of Medicine
in conjunction with the
Faculty of Graduate Studies

Towards a Better Treatment of Parkinson's Disease

by

Bradley Darryl Karain

A Dissertation submitted in partial satisfaction of
the requirements for the degree of
Doctor of Philosophy in Microbiology and Molecular Genetics

March 2014

Each person whose signature appears below certifies that this dissertation in his/her opinion is adequate, in scope and quality, as a dissertation for the degree Doctor of Philosophy.

_____, Chairperson
Wei-Xing Shi, Professor of Pharmaceutical and Administrative, and Basic Sciences, Schools of Pharmacy and Medicine

_____
Eileen Brantley, Assistant Professor Pharmaceutical and Administrative, and Basic Sciences, Schools of Pharmacy and Medicine

_____
Richard Hartman, Associate Professor of Psychology, School of Behavioral Health

_____
Mark Johnson, Associate Research Professor of Microbiology and Molecular Genetics, School of Medicine

_____
Ubaldo Soto-Wegner, Assistant Research Professor of Microbiology and Molecular Genetics, School of Medicine

ACKNOWLEDGEMENTS

I would like to express my deep gratitude to Dr. Shi for his enormous investment of valuable time, resources, and energy in helping me to achieve my academic goals. My understanding of the scientific method has vastly matured from the student who entered this lab several years ago. Your patience and deep, deep knowledge of not just neuroscience, but of science and mathematics in general, are qualities I will always try hard to emulate.

I would like to thank my committee members for constant encouragement and succinctly brilliant advice. Dr. Mark Johnson, Dr. Eileen Brantley, Dr. Ubaldo Soto-Wegner, Dr. Richard Hartman: thank you for always showing an interest, for your brilliant guidance, and frankly for continually inspiring me simply to persevere to the end.

To my lab-mates, family, and friends I would simply like to say thank you. Your constant support has been invaluable in advancing me towards this goal.

I wish to express my gratitude to Jinglei Wang (for image analysis) and Nhi Ngo and Angelica Rabanal for their work in immunofluorescence, used to produce a confocal microscopy image at the LLUSM Advanced Imaging and Microscopy Core.

Special thanks to Sonjia Dennis for assistance with electrophysiological and behavioral studies. Indeed, the behavioral studies could not possibly have been completed in the necessary time frame without her involvement.

This work was supported in part by DA 032857 (WXS), NSF Grant No. MRI-DBI 0923559 (SMW), and Loma Linda University School of Pharmacy.

CONTENTS

FIGURES

ABBREVIATIONS

DA	Dopamine
6-OHDA	6-Hydroxydopamine
L-DOPA	L-3,4-Dihydroxyphenylalanine
GP	Globus Pallidus
SNc	Substantia Nigra Pars Compacta
FFT	Fast Fourier Transform
HT	Hilbert Transform

ABSTRACT OF THE DISSERTATION

Towards a Better Treatment of Parkinson's Disease

by

Bradley Darryl Karain

Doctor of Philosophy, Graduate Program in Microbiology and Molecular Genetics
Loma Linda University, March 2014
Dr. Wei-Xing Shi, Chairperson

Current therapies for Parkinson's Disease, the second most common neurodegenerative disorder, do not prevent disease progression, and induce extremely detrimental side-effects. Improving the best current pharmacological therapy, L-DOPA, carries important clinical benefits, partly by reducing the dose-related side-effects which occur after five to ten years of use. **Thus the central aim of this proposal is to determine whether low doses of a D2 antagonist may, by selectively blocking the dopamine autoreceptor-mediated feedback inhibition of dopamine neurons, potentiate L-DOPA's effect on individual basal ganglia neurons and its antiparkinsonian effects in Parkinsonian animals.**

Electrophysiology (extracellular single-cell recording in the globus pallidus) and behavioral (cylinder test) studies were performed to determine if co-administration of a small dose of the D2 antagonist raclopride with L-DOPA results in an enhanced therapeutic effect of L-DOPA in 6-OHDA lesioned (parkinsonian) rats.

Preliminary data revealed different subgroups of pallidal neurons, with different responses to L-DOPA injection. However, we showed that a major method by which sub-groups of pallidal neurons have been identified in previous studies was unreliable, halting further study of L-DOPA's effect on different subgroups of pallidal neurons using that method. Thus, we focused on classification of pallidal neurons and the changes of these neurons in Parkinsonian animals. Previous studies report pallidal neurons as

Type-I (negative initial peak) or Type-II (initial positive peak). Our studies suggest electrode impedance determines whether the recorded waveform is Type-I (low impedance electrode) or Type-II (high impedance electrode). Pallidal neurons can be more reliably classified based on functional connectivity with cortical neurons. More importantly, our findings showed that, in Parkinsonian rats, pallidal neurons positively coupled to cortical activity usually lag, while in control rats close to half of pallidal neurons lead cortical activity. Also, we found significantly increased cortical control of pallidal neurons in Parkinsonian rats indicated by a significant increase in the observed number of pallidal cells negatively coupled to cortical activity. The quantity of pallidal neurons uncoupled to cortical activity was observed to significantly decrease in 6-OHDA lesioned rats compared to controls.

Behaviorally, raclopride (5 μg/kg, i.p.) was found to significantly potentiate the therapeutic benefit of L-DOPA (3 mg/kg, i.p.).

CHAPTER ONE

THE EXTERNAL GLOBUS PALLIDUS IN PARKINSON'S DISEASE: DA AUTORECEPTOR SUPPRESSION AND POTENTIAL FOR POTENTIATION OF L-DOPA'S THERAPEUTIC BENEFIT

Abstract

Parkinson's Disease (PD) is a neurodegenerative condition characterized by the loss of dopamine producing cells in the substantia nigra (SN). The most obvious and early symptoms of the disease occur due to the loss of dopamine (DA) innervation in groups of subcortical nuclei known as the basal ganglia (BG). These nuclei include the striatum (Str), globus pallidus internus (GPi) and globus pallidus externus (GPe). Different subgroups of globus pallidus (GP) neurons are likely to have different functional roles, and several methods exist for identifying heterogeneity among pallidal neurons, including differences among action potential shape. We consider effects on the GP of the major afferent (glutamatergic from the subthalamic nucleus (STN) and GABAergic from the Str) and efferent (GABA to all basal ganglia nuclei) projections. The cortex has a large indirect influence due to glutamatergic cortical projections to both the Str and STN. DA and DA agonists have a critical modulatory influence on GP activity through opposite effects on the largely independent BG pathways referred to as 'direct' and 'indirect'. The Str medium spiny neurons (MSN) in the 'direct' pathway express Gs-coupled D1 receptors and activation of the direct pathway facilitates movement, whereas the 'indirect' pathway Str MSNs express Gi-coupled D2 receptors and activation of the indirect pathway inhibits movement. DA autoreceptors are DA receptors expressed on DA neurons. They are D2-like and highly sensitive to small doses of DA agonists with raclopride being a highly specific D2 antagonist. The specific aims explored are 1) identify GP neuron subgroups in isoflurane-anesthetized rats using previously described classification schemes, one based on shape of the extracellular waveform and another based on functional connectivity between GP and cortical neurons, and quantify changes in these groups following DA depletion 2) test the hypothesis that low doses of raclopride selectively block DA autoreceptors and potentiate the therapeutic effect of L-DOPA on behavior.

Parkinson's Disease and Movement Control

PD was first described 200 years ago, yet remains the second most common neurodegenerative disorder, with no clear path for prevention or cure. The pathological hallmark of PD is the death of DAergic neurons in the SN that innervate a complex and highly interconnected group of subcortical nuclei known as the basal ganglia (BG). The BG are intimately involved in control of movement[1] and may be considered to consist of three components. First, the input nuclei comprised of the caudate nucleus and the putamen, collectively referred to in rats as the striatum (Str). Next is the output nucleus, the internal segment of the globus pallidus (GPi), referred to in rats as the entopeduncular nucleus. The substantia nigra pars reticulate (SNr) is also an output nucleus but is located at the base of the midbrain, some distance from the BG. Lastly is the intrinsic nucleus, the external segment of the globus pallidus (GPe) referred to in rats simply as the GP. The activity of the GPe is strongly influenced by the subthalamic nucleus (STN) and the substantia nigra pars compacta (SNc), though again these nuclei are located some distance from the BG.

The BG of the rat evinces conscious movement control due to the activity of approximately 26,000 DA neurons in the SNc extensively innervating the Str. The left diagram in Fig. 1.1 [2] is a simplified diagram of the functional organization of the BG. Red arrows indicate glutamatergic (excitatory) inputs, blue arrows indicate GABAergic (inhibitory) inputs, and the grey arrow is DAergic. The diagram on the right in Fig 1.1 shows localization of the BG in the human. Ninety percent of Str neurons are MSNs (the other 10% being interneurons), divided into the D1R-expressing neurons giving rise to the direct pathway (Fig. 1.1: Str → GPi/SNr). and D2R-expressing neurons of the indirect pathway (Fig. 1.1: Str → GPe → STN → GPi/SNr) [2]. Each DA axon innervates approximately 75,000 MSNs, with each MSN innervated by 95 to 194 DA neurons [3]. In

humans each DA neuron innervates as many as 1 million MSNs. The modulatory influence of DA is thought to occur in part by an excitatory influence on MSNs expressing D1 receptors (Gs-coupled) and an inhibitory influence on MSNs expressing D2 receptors (Gi-coupled)[3].

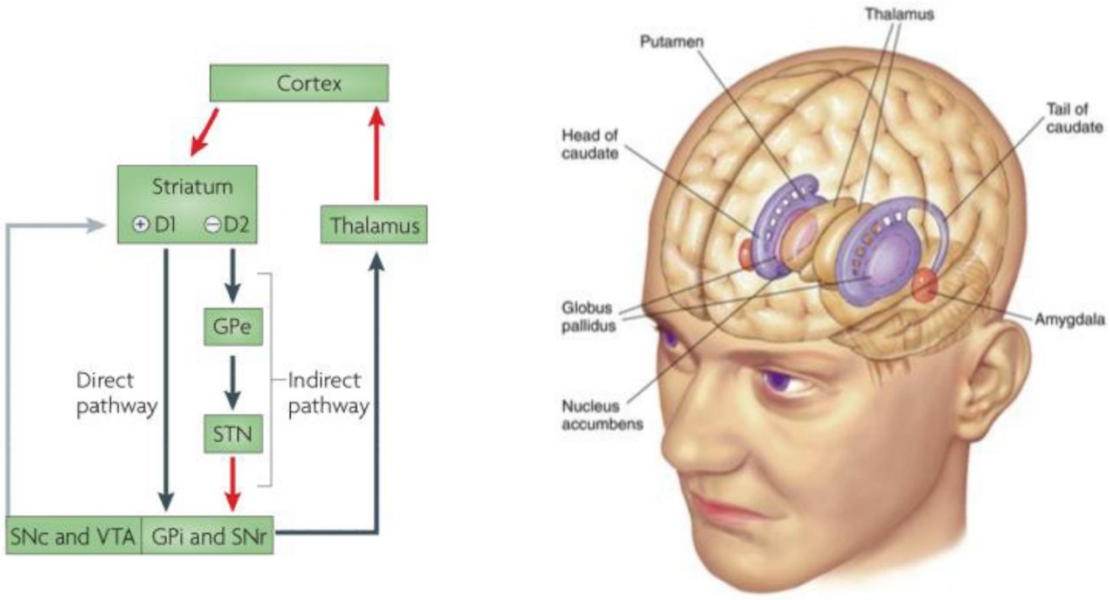

Figure 1.1 Organization of the Basal Ganglia

Importance of the GP

Pallidal projection neurons are GABAergic, 1/3 of which project exclusively back to the Str. GPe neurons project to many subcortical regions including the GPi, STN, and SNr) [3, 4]. Reciprocal connections between the GP and other BG nuclei indicate that

the GP plays a significant role in modulating neuronal activity of the entire BG; in turn, the activity of GP neurons is coordinated by several major inputs that involve the Str [5]. Early BG models considered the GP to be a homogeneous relay nucleus, simply passing striatal information to the subthalamic nucleus (STN) and BG output nuclei. In fact, the GP appears to be a diverse structure that performs complex computations within its borders [6]. Also, the Str and GP are both post-synaptic to DA neurons, but GP neurons fire tonically at a relatively high frequency compared to Str neurons [7]. Thus, as an important integrator of BG activity with numerous feedback loops, coupled with a faster firing rate than Str neurons, GP neurons are a preferred target to study effects of drugs on the BG electrophysiologically.

Afferent Glutamatergic Projections

STN neurons are glutamatergic, and occupy a pivotal position in the circuitry of the BG. They receive direct excitatory input from the cerebral cortex and the thalamus, and directly excite the GABAergic BG output neurons in the GPi and the SNr. They are also engaged in a reciprocal synaptic arrangement with GABAergic neurons in the GPe. STN lesions reduce bursting in normal rats and normalize the firing pattern in the GP of rats with 6-OHDA lesions, suggesting the STN is important in modulation of the pattern of activity of GP neurons. This may account for the therapeutic effect of STN lesions in Parkinson's disease [8]. One of the functions of the excitatory glutamatergic STN is to relay cortical activity to other basal ganglia structures. The response of the STN to cortical input is influenced by GABAergic inhibition from the reciprocally connected GP. STN and GP activity is intimately related to cortical activity. The oscillatory activity of the STN-GP network is regulated in a complex manner, with the cortex possibly driving oscillatory activity observed in disease states [9].

Animal models of parkinsonism have shown that excitatory corticosubthalamic input, during periods of synchronized bursting activity, are partly responsible for driving changes in neuronal GP activity [10]. However, the increased activity of STN neurons following a midbrain dopaminergic lesion cannot be due solely to inhibition-disinhibition involving the striato-pallido-subthalamic pathway and induced by striatal DAergic depletion [11].

There are approximately 46,000 GPe neurons in the rat [12], able to fire autonomously and requiring no external source for maintenance. However, neuronal reactivity in the BG network considerably differs between early and late stage models of PD. Severe lesions induce pathological activity of STN neurons not mediated by the GP. STN hyperactivity is a cause of the unchanged GP neuron activity. In the GP-STN-GP network, the excitatory influence of the STN-GP pathway overrides that of the GABAergic GP-STN pathway [13].

Afferent GABAergic Projections

GP neurons in 6-OHDA-treated hemi-parkinsonian rats fire significantly more strong bursts than in normal rats. DA-depletion increases burst firings of striatal (Str) neurons projecting to the GP and the increased Str-GP burst inputs play a significant role in the generation of pauses and bursts in GP and its projection sites. Striatal muscimol injection in 6-OHDA-lesioned rats increases firing rate, with reduced pauses and bursts in the GP. Str projection neurons in control rats have very low spontaneous activity, whereas DA-depletion causes Str neurons to exhibit stronger bursts and a higher firing rate, most of which are MSNs projecting only to the GP. Thus, DA-depletion increases burst firing of Str neurons projecting to the GP and increased Str-GP burst inputs play a significant role in the generation of pauses and bursts in GP.

Therapeutic reduction of bursting in Str-GP inhibitory inputs may help reduce PD dysfunction [14].

Slow oscillatory activity emerges in BG nuclei in anesthetized rats after DA cell lesion. Unilateral DA cell lesion induces a striking ipsilateral increase in incidence of slow oscillations (0.3-2.5 Hz) in firing rate in STN, GP, and SNr. Phase relationships assessed through paired recordings using SNr LFP as a temporal reference show that slow oscillatory activity in GP spike trains is predominantly antiphase with Str oscillations, while STN slow oscillatory activity is in-phase with the cortex but antiphase with the GP. Thus, following DA lesion, increased oscillatory activity in GP spike trains is shaped more by increased phasic inhibitory input from the Str than by phasic excitatory input from the STN. Also, oscillatory activity in SNr spike trains is typically antiphase with GP oscillatory activity and in-phase with STN oscillatory activity. Increased oscillatory activity in the GP is facilitated by an effect of DA loss on Str 'filtering' of slow components of oscillatory cortical input. Increased oscillatory activity in STN spike trains is supported by convergent antiphase inhibitory and excitatory oscillatory input from GP and cortex, respectively. Increased oscillatory activity in SNr spike trains is driven by convergent antiphase inhibitory and excitatory oscillatory input from GP and STN, respectively [15].

Str and GPe neurons fire synchronously following acute and repeated DA blockade. Although phase lags between neuronal discharges in the GPe and Str are uniformly distributed prior to DA blockade, Str significantly lags GPe discharges after repeated DA blockade. Acute DA blockade is sufficient to produce synchronous oscillatory activity across BG neuron populations, and prolonged DA blockade results in phase lag changes in pallidostriatal synchrony [16].

Classification of GP Neurons

Several systems have been introduced to describe the heterogeneity of GP neurons. Kita and Kitai describe three distinct electrophysiological groupings in the adult rat: continuous repetitive firing (more than 70%), burst firing neurons, and a few non-firing neurons [7]. Alternatively, Nambu et al. describes three different types of neurons in brain slices from adult guinea pigs: At the resting membrane potential, Type I neurons (56%) are approximately 40 x 23 μm , Type-II neurons (37%) are approximately 29 x 17 μm, and Type III neurons (7%) which are approximately 18 x 12 μm. The morphological differences are supported by numerous electrophysiological differences. Type-I and II were shown to be projection neurons while Type III were small interneurons [17, 18]. Cooper et al. describe GP neurons in three subgroups based on both electrophysiological properties and morphology of biocytin-filled neurons. Type A neurons (63 %), Type B neurons (32 %), and Type C (5 %). The rarely encountered type C cells are believed to be large cholinergic neurons [19]. These results confirm neuronal heterogeneity in the adult rodent GP. However, a GP neuron subtype identified in one study is often not easily identified in another study. For example, the Type III cells identified by Nambu et al. [17, 18] are not found at all by Cooper et al [19].

Waveform Classification

A classification scheme based on extracellular waveform properties was used in 1995 by Kelland et al [20]. Extracellular single-unit recording techniques were used to examine the rat GP. Two distinct biphasic extracellular waveforms were observed in both paralyzed and ketamine-anesthetized rats, Type-I (negative/positive waveform) and Type-II (positive/negative waveform). A higher mean firing rate, with significantly slower conduction velocities, was found in Type-II neurons compared to Type-I. The most striking pharmacological difference Kelland et al. found was that the mixed DA agonist

apomorphine inhibited Type-I GP neurons, where previous studies repeatedly found Type-II GP cells to be excited by the same treatment.

Pretreatment with a subthreshold dose of apomorphine reduced the responsiveness of Type-I and Type-II cells to a subsequent high dose of apomorphine. However, pretreatment with the NMDA antagonist dizocilpine (MK801) produced a significant change in the pattern of response to apomorphine for Type-II GP neurons only. Relative to observations in locally anesthetized, paralyzed rats, ketamine anesthesia reduced the firing rate of both cell types, but did not significantly alter their direction of response to apomorphine. This suggested the existence of two GP cell types with distinct extracellular waveforms and opposite responses to dopamine receptor stimulation [20].

Classification by Functional Connectivity

The cause of abnormal oscillatory synchrony in PD remains unclear. Nonlinear time series analyses and information theory capture the effects of dopamine depletion on directed information flow within and between the STN and GP. Neuronal activity recorded simultaneously from these nuclei in 6-OHDA-lesioned Parkinsonian rats, and compared to that in DA-intact control rats, shows that lesioning increased beta-frequency (~20 Hz) oscillations and information transfer between STN and GP neurons. Temporal profiles of the directed information transfer supported the neurochemistry of these nuclei, "excitatory" from STN to GP and "inhibitory" from GP to STN. The GP of lesioned animals consists of "type-inactive" (GP-TI) and "type-active" (GP-TA) neurons, with the firing preferences revealing distinct temporal profiles of interaction with STN and each other. GP-TI neurons output is of greater causal significance than that of GP-TA neurons for the reduced activity that periodically punctuates the spiking of STN neurons during beta oscillations. A key driver for recruiting GP-TI neurons (but not GP-TA) was

the STN. Short-latency interactions between GP-TI and GP-TA neurons suggested mutual inhibition. Information flow around the STN-GP circuit is found to be exaggerated in Parkinsonism [21].

Different striatal projection neurons create a dual organization essential for basal ganglia function. Similarly, there exists an analogous division of labor in the GP of Parkinsonian rats. The characteristics of GP-TA and GP-TI neurons are maintained by distinct molecular profiles and axonal connectivities. GP neurons firing antiphase to STN neurons often express parvalbumin and target downstream BG nuclei, including STN. In contrast, GP neurons firing in-phase with STN neurons, express preproenkephalin and only innervate the Str. This novel cell type provides the largest extrinsic GABAergic innervation of the Str, targeting both projection neurons and interneurons. The two GP neuron populations together orchestrate activities across all basal ganglia nuclei in a cell-type-specific manner [22].

Modulatory Role of Dopamine

DAergic cells are six to ten times more sensitive to DA and DA agonists [23] than most Str cells. This differential sensitivity of DA auto- and postsynaptic receptors may explain the apparently paradoxical behavioral effects induced by small compared to large doses of some DA agonists [23, 24]. DA receptors occur in five subtypes (D1 through D5) grouped into two families, D1-like and D2-like, commonly referred to simply as D1 and D2 DA receptors. Of the many D2 antagonists available, raclopride has a high D2 receptor specificity in the rat brain both in vitro and in vivo, and is a useful tool to study DA D2 receptors [25-27]. The plasma half-time of raclopride is short in the rat (about 40 min), and high in man (about 14 hours) [28].

Synergistic effects are exerted on firing rates of BG neurons and on the expression of stereotyped behavior in rats, evidenced by the attenuation of D2

agonist effects in the absence of endogenous dopamine [29]. Dopamine, via D2 receptors, inhibits striatopallidal activity, resulting in a disinhibition of neurons in GP [30]. DA and DA agonists may affect BG function by modulating GABAergic transmission in the GP [31].

DA acts on presynaptic D2 receptors on striatopallidal terminals to reduce the release of GABA in the GP. Attenuation of this mechanism following the depletion of DA may contribute to the changes in GP neuronal activity observed in animal models of PD [32].

DA modulates multisecond oscillations in GP activity, while tonic DAergic and glutamatergic transmission is necessary for normal slow oscillatory function [33, 34]. For instance, the mixed DA agonist apomorphine causes an increase in the unit activity of spontaneously firing neurons in the rat GP [35]. Interestingly, the psychostimulant d-amphetamine causes a significant increase in the unit activity of spontaneously firing neurons in the rat GP [36]. The time schedule of drug administration is critical, as a nonexcitatory 'priming' dose attenuates the significant increase in unit activity of rat GP neurons [34, 37]. Blocking D1 receptors attenuates the postsynaptic, but not autoreceptor-mediated (or D2) effects of dopamine agonists [38]. Stimulation of both receptor subtypes is necessary for full expression of postsynaptic receptor-mediated effects of DA and DA agonists in the BG [39-41]. The denervated DA receptors in rats with unilateral nigrostriatal lesions, or the processes they mediate, change such that they no longer have the requirement seen in controls for concurrent stimulation of the complementary DA receptor subtype for expression of the selective agonist effects [42]. The changes in rate and entrainment to the LFP observed in MSNs after DA depletion are somewhat dissociable, and lack of D1- or D2-type receptor activation can exert independent yet interactive pathological effects during the progression of PD [43].

Following DA depletion, there is an increase in the expression of $GABA_A$ and $GABA_B$ receptors and the ratio of AMPA to NMDA receptors. The autonomous activity of GPe neurons declines following DA depletion [12]. Tonic stimulation of AMPA receptors plays an important role in maintaining the basal activity of GP neurons and in mediating the effects of increased excitatory input from STN afferent neurons [44].

Postsynaptic D2-like receptors are functionally expressed on GP cell bodies and may supersensitize following DA-denervation. A direct D2 modulation of calcium conductance in the GP may alter GP firing properties and GABA release onto pallidofugal targets [45]. DA modulates coherent oscillatory activity in the BG, and through the STN shapes the effects of DA receptor stimulation on BG output [46].

DA D1 receptors potentiate D2 receptor effects. The similar actions of partial and full D1 agonists support evidence for a D1 receptor reserve and possibly an effector system other than adenylate cyclase [47]. The GP exerts significant control over the firing rate and pattern of SNc DAergic neurons through a disynaptic pathway involving SNr GABAergic neurons [48] and is at least one important way in which local application of the $GABA_A$ antagonist bicuculline induces burst firing of dopaminergic neurons (through disinhibition of this tonic inhibitory input) [49].

A combination of direct and indirect influences ultimately determines the impact that an activated DAergic system has on pallidal brain regions [50]. Both glutamate and acetylcholine appear to play a role in DAergic modulation of Str and GP activity [51]. Tonically active DA neurons, probably acting through the striatopallidal pathway, regulate the activity of GP neurons [52]. Striatopallidal neurons contribute to the excitatory effect of apomorphine on the activity of pallidal neurons in normal animals [53]. However, DAergic influences reduce the flow of information from the cortex to the pallidum, which may constitute a focusing mechanism by which only information from the

strongest cortical inputs would pass to the pallidum, with less prominent activity disregarded [54].

The DAergic control of multisecond oscillations in GP firing rate demonstrates D1/D2 receptor synergism, in that the effects of D1 agonists are potentiated by and partially dependent on D2 receptor activity. Modulation of multisecond oscillations in firing rate represents a means by which DA can influence GP physiology [55].

Collaterals of SNc DAergic axons project to the Str and GP. Further, DA plays a role in the modulation of the firing rate but not the firing pattern of GP neurons. DA depletion in the SNc-GP DAergic pathway may play a role in the development of motor dysfunction [56].

Autonomous GPe pacemaking, normally serving to desynchronize activity, declines in Parkinsonian mice. This is attributable to the downregulation of the hyperpolarization and cyclic nucleotide-gated (HCN) channel, an ion channel essential to pacemaking. Viral delivery of HCN2 subunits are shown to restore pacemaking and reduced burst spiking in GPe neurons. However, the motor dysfunction induced by DA depletion is not reversed, suggesting that pacemaking loss is a consequence, not a cause, of key network pathophysiology [57].

In extracellular single-unit recording studies in awake, immobilized rats, many tonically active neurons in the entopeduncular nucleus, GP, and SNr have multisecond slow oscillations in the firing rate. There is significant structure in BG neuron spiking activity at unexpectedly long time scales, as well as a novel effect of DA on firing pattern in this slow temporal domain. The modulation of multisecond periodicities in firing rate by DAergic agonists suggests the involvement of these patterns in behaviors and cognitive processes that are affected by DA. Periodic firing rate oscillations in BG output nuclei should strongly affect the firing patterns of target neurons and are likely involved in coordinating neural activity responsible for motor sequences. Modulation of slow,

periodic oscillations in firing rate may be an important mechanism by which DA influences motor and cognitive processes in normal and pathological states [58]. Burst firing in DAergic neurons leads to an increase in extracellular DA levels in the Str when compared with less bursty patterns with similar overall firing rates [59]. Striatonigral and striatopallidal neurons differentially modulate motor behavior under normal and pathological conditions [60].

The pallidal disynaptic disinhibitory control of the dopaminergic neurons dominates the monosynaptic inhibitory influence because of a differential sensitivity to GABA of the two nigral neuron types. Nigral GABAergic neurons are more sensitive to $GABA_A$ mediated inhibition than DAergic neurons, in part due to a more hyperpolarized $GABA_A$ reversal potential. The more depolarized $GABA_A$ reversal potential in the DAergic neurons is due to the absence of KCC2, the chloride transporter responsible for setting up a hyperpolarizing Cl(-) gradient in most mature CNS neurons. In addition to the effects that nigral GABAergic output neurons have on their target nuclei outside of the BG, local interactions between GABAergic projection neurons and DAergic neurons are crucially important to the functioning of the nigral DAergic neurons [61].

6-OHDA lesions provide a model of progressive DA neuron degeneration in the rat, useful for exploration of neuroprotective therapies and to study mechanisms of functional and structural recovery after partial damage of the nigrostriatal DA system [62].

The GP sends a significant GABAergic projection to the thalamic reticular nucleus. DA controls the activity of the thalamic reticular neurons by regulating the inhibitory input from the GP [63].

Motor dysfunction may be caused by DA-depleted BG abnormally processing information originating from the massive projections of the motor cortex (MC). Following DA-depletion, the spontaneous firing of Str-GPe neurons increases, and MC stimulation

evokes a shorter latency excitation followed by a long-lasting inhibition not normally visible. The increased firing activity and the newly visible long inhibition generate tonic inhibition and a disfacilitation in GP. The disfacilitation in the GP generates a powerful long inhibition in the GPi. Motor dysfunction in PD is partially due to the generation of abnormal response sequences in the BG. Interestingly, intra-striatal DA supplements effectively suppress abnormal signal transfer [64].

Relationship to Cortical Activity

Oscillatory processes at the levels of single neurons and neuronal networks in the STN and GP are associated with the operation of the BG. Abnormal low-frequency rhythmic bursting in the STN and GP is characteristic of PD, whereas autonomous oscillation of STN and GP neurons underlies tonic activity and is important for synaptic integration. The BG uses both the pattern and the rate of neuronal activity to encode information. In the DA-depleted state the STN and GP are more sensitive to cortical oscillation [65]. Cortical activation drives individual pallidal neurons which may in turn influence GABAergic interneuron activity of the neostriatum while simultaneously patterning neuronal activity in the BG downstream of the neostriatum [66]. Both the rate and pattern of activity of STN and GP neurons are profoundly altered by chronic DA depletion. Furthermore, the relative contribution of rate and pattern to pathological information transfer is closely related to cortical activity [67]. Coherent oscillatory activity is present at the level of LFPs recorded in cortico-BG circuits and synchronized population activity is dynamically organized according to brain state, frequency, and nucleus. In these brain circuits, synchronized activity is a potential mechanism underlying functional organization [68].

It is unclear what modifications of neuronal activity underlie the clinical manifestations of PD and the efficacy of antiparkinsonian pharmacotherapy. Studies

suggest release of GABAergic striatopallidal neurons from D2 receptor-mediated inhibition allows spreading of cortical rhythms to the GP in rats with 6-OHDA-induced nigrostriatal lesions. Two neuronal populations coexist in the GP of 6-OHDA-lesioned rats, but have opposite phase relationships with cortical and Str activity. 'Inverse-phase' GP neurons exhibit reduced firing coupled to Str activation during slow waves, suggesting GP oscillation driven by striatopallidal hyperactivity. Spreading of inverse-phase oscillations through pallidonigral axons might contribute to the abnormal 'direct-phase' cortical entrainment of BG output. Abnormal slow rhythms may promote enduring changes in functional connectivity along the striatopallidal axis, contributing to D2 agonist-resistant clinical signs of parkinsonism [69].

Inappropriately synchronized beta oscillations (15-30 Hz) in the STN accompany movement difficulties in PD. The cellular and network substrates underlying these exaggerated beta oscillation remains unclear. However, GP activity, forming a pacemaker network with the STN, might be of particular importance. GP neurons, by virtue of their spatiotemporal synchronization, widespread axon collaterals and feed-back/feed-forward mechanisms, are well placed to orchestrate and propagate exaggerated beta oscillations throughout the entire BG in PD [70].

Human Studies

Current hypotheses of BG dysfunction in PD suggest that neuronal hypoactivity in the GPe, and hyperactivity in the output nuclei (GPi and SNr), result in the cardinal symptoms of PD. The therapeutic effect of the mixed DA agonist apomorphine results from a normalization of the imbalance of neuronal activity in the direct and indirect pathways [71]. A decreased motor response after repeated doses of apomorphine is observed in severely affected PD patients. Fast postsynaptic desensitization to DA agonists may take place in the BG nuclei and play a role in the physiopathology of L-

DOPA long-term treatment syndrome [72]. However, apomorphine-induced reduction of parkinsonian symptoms is not solely due to a decrease in overall activity in the GPi or STN as predicted by the current model of BG function in PD [73].

The BG may receive multiple cortical inputs at frequencies <30 Hz and, in the presence of DAergic activity, produce a high frequency drive back to the cerebral cortex [74]. Neurons in the motor territories of the GPe and GPi respond to cortical stimulation. Response patterns observed in PD patients are combinations of an early excitation, an inhibition, and a late excitation. Many GPe and GPi neurons of the PD patients showed burst or oscillatory burst activity [75].

Primate Studies

MPTP treatment changes the pattern of activity and synchronization in the GPe and GPi. These changes are related to the symptoms of PD and especially to the parkinsonian tremor [76]. Extracellular recordings in primates have identified two types of neurons in the GPe: high frequency pausers (HFP) and low frequency bursters (LFB). The differences are possibly related to underlying cellular properties which are fundamentally different [77]. Two distinct neuronal populations exhibit firing-pattern characteristics conserved between species, although the firing rate is significantly lower in rats than in primates. Significant differences in waveform duration and shape are insufficient to create a reliable waveform-based classification in either species [78].

The pattern of activity of GPe neurons is tightly regulated by GABAergic inhibition. In addition to extrinsic inputs from the Str, the other source of GABA to GP neurons arises from intrinsic intranuclear axon collaterals. Also, increased intranuclear transmission promotes resetting of autonomous activity and rebound-burst firing following DA depletion. This suggests that intranuclear synaptic transmission is

augmented by chronic DA depletion which could contribute to the aberrant GP neuronal activity observed in PD [79].

Lesions involving the nigrostriatal pathway change the firing patterns but not the mean firing rates of pallidal neurons. In lesioned monkeys pallidal neurons fire in bursts continuously: during movement, rest and sleepiness. The bursting pallidal activities are likely a consequence of the interruption of the nigrostriatal DAergic pathway [80].

Abnormalities exist in the spontaneous activity of GP neurons at the output of the basal ganglia, with the mean spontaneous firing rate of GPi neurons increased and GPe decreased. Shorter spike intervals, suggesting increased excitation, are seen in both the GPi and GPe. However, the proportion of spike intervals longer than 100 ms increased in the GPe but remained unchanged in the GPi, suggesting increased inhibition only in the GPe. In the two populations, bursting activities and the mean variability of firing rate increased. Intensity of the changes varied with time and severity of the nigral lesion. In severe parkinsonism, the neuronal activity at the output of the basal ganglia is excessive [81].

Filion et al. [82] injected cynomolgus monkeys with the mixed dopamine agonist apomorphine, before and after they were rendered parkinsonian. Nearly all GPi neurons decreased their firing rate following apomorphine, with the opposite effect in the GPe. Identical doses of apomorphine were seen to effect a large variation between neurons in firing rate change. When the changes in firing rate were moderate or null, abnormal bursting firing patterns were normalized. LFB neurons showed decreased firing rate following apomorphine.

After being rendered parkinsonian, many pallidal neurons (35%) become oscillatory, and 19% of pallidal pairs have oscillatory cross-correlograms, supporting the model of parallel processing in the BG of normal monkeys and suggesting a breakdown of the independent activity in the parkinsonian state [83]. Boraud et al. found, following

parkinsonism, a decrease in firing rate and a slight increase in bursting activity of GPe neurons [84]. The GPi showed a considerable increase in both firing frequency and the number of bursting cells. L-DOPA treatment left the GPe firing pattern unchanged, while the GPi showed decreased firing frequency (even below control level) and slightly reduced bursting activity.

Abnormal cortical firing patterns and synchronization, rather than reduced firing rates, may underlie PD akinesia and persistent muscle rigidity [85].
After parkinsonism, firing rates decrease in the GPe and increase in the GPi. A reversal of these rate changes occurrs during the "on" periods of DA replacement therapy. Changes in both pallidal discharge rates and synchronization are correlated with the clinical manifestations of parkinsonism and its pharmacological treatment [86].

Hong et al. found that multisecond oscillations commonly occur in primate BG neurons and are unchanged by parkinsonism [87]. The GPi may initiate reward-related signals through its effects on the lateral habenula, which then influences the DAergic and serotonergic systems [88]. Reduced GPe activity alone does not produce parkinsonism. Other changes, such as altered discharge patterns in STN and GPi, may play an important role in the generation of parkinsonism [89].

Cylinder Test

PD is primarily identified as a movement disorder. Thus, any animal model will require sensitive behavioral tests to determine both motor impairment and therapeutic benefit, if any, according to treatment regimen. The animal behavior correlates in PD may be investigated in several ways. The rotarod and cylinder test reveal significant motor impairment, but only the cylinder test reveals improvement due to dopaminergic drugs [90]. The cylinder test, a modification of a test first described in 1990 [91] has been found to have the ability to detect even mild neurological impairments [92].

Effect of L-DOPA

Though long-term use of L-DOPA evokes dyskinesia through striatal site-specific mechanisms [93], L-DOPA remains the most effective pharmacological treatment for the motor dysfunctions of PD. L-DOPA, as a DA precursor, increases DA synthesis and release. This increased stimulation of postsynaptic DA receptors, coupled with simultaneous interference with the DA autoreceptor negative feedback mechanism could be an important approach for alleviation of Parkinsonian symptoms [94].

The hypothesis of this proposal is that low doses of raclopride (a D2 antagonist) selectively blocks DA autoreceptors and potentiates L-DOPA's effects on neurons postsynaptic to DA terminals including GP neurons.

This hypothesis is based on the observation that low doses of D2 agonists selectively activate D2 autoreceptors on DA neurons without significantly affecting D2 receptors on DA target neurons. Since activation of D2 autoreceptors inhibits DA release, blockade of these receptors by low doses of a D2 antagonist would enhance the effect of L-DOPA on DA target neurons. If this hypothesis proves to be correct, co-administration of a low dose of a D2 antagonist may reduce the dose of L-DOPA required to produce therapeutic effects, thereby delaying the onset of undesirable side effects of L-DOPA. The latter have been shown to be dose-dependent. In order to test this hypothesis, experiments were planned to test the electrophysiological effect of L-DOPA on GP neurons and compare the effect to that of L-DOPA plus raclopride. However, in pursuit of this investigation, the first set of experiments explored the effect of L-DOPA on GP neurons, compared to the effect of L-DOPA co-administered with a low dose of the highly selective D2 antagonist raclopride.

Preliminary results with L-DOPA indicated the firing rate of GP neurons often increased, but also sometimes decreased, surprising since early studies of non-selective DA agonists on GP neurons typically show a significant increase in the activity of GP cells [29, 34, 35, 37, 39]. One reason for the discrepancy may be due to earlier studies averaging the effect seen on all GP neurons. More recent studies reveal a more nuanced breakdown of specific responses of GP neurons to non-selective DA agonist administration [20, 50]. Indeed, Kelland et al. found the firing rate of roughly half of GP cells to increase and half to decrease [20].

One of the main methods Kelland et al. used to distinguish GP neuron subtypes was the shape of the extracellularly recorded waveform, type-I with a negative initial peak and type-II with a positive initial peak [20]. The existence of GP neuron subtypes, with distinctly different responses to non-selective DA agonists, suggested the exploration of the response of GP neurons to L-DOPA should be delayed until we first obtained a more detailed characterization of GP cells themselves. Accordingly, the electrophysiological protocol was altered so that the subtypes described by Kelland et al. could be verified. Using the same experimental conditions as Kelland et al., we reproduced the results of Kelland.

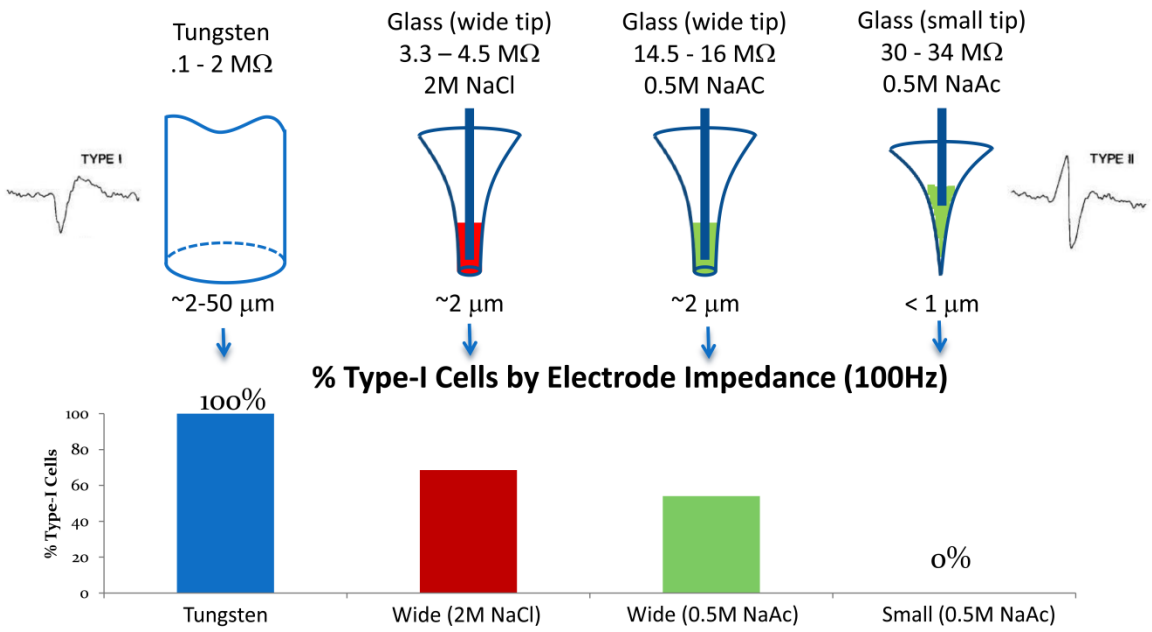

Figure 1.2 Electrode Impedance Effects on Waveform Shape

However, our results reveal information not evident in the results of Kelland et al. Fig 1.2 shows that small-tip, large impedance electrodes record waveforms as Type-II whereas large-tip, small impedance electrodes preferentially record waveforms as Type-I, so we were able to show that one of the main findings of Kelland, that GP neurons may be distinguished based partly upon the spike shape was in fact an unreliable measure.

While Kelland et al. used ketamine (an injectable anesthetic), we chose to use isoflurane (an inhaled anesthetic). Injected anesthetics are generally given in a bolus dose, then supplemented as necessary, so the animal has widely varying plasma levels of anesthetic. Isoflurane, being inhaled, reaches a steady state level far faster and is easily adjusted so that only the minimum required dose is administered.

However, it is possible to classify GP neurons in another way. During the course of verifying the results of Kelland et al. another classification system was also confirmed.

A second recording electrode was placed in the cortex, and a classification of GP neuron subtypes based on functional connectivity between the GP and the cortex was observed, in agreement with previous studies (which used urethane, another injectable anesthetic) [22, 69]. With no clear evidence linking these disparate classification systems, the experimental design was altered to first characterize GP neurons. Only then could the effort be made to determine how different GP subtypes would respond to L-DOPA. Given this requirement, the following specific aims are designed to test the hypothesis.

Specific Aims

Specific Aim 1

Identify GP neuron subgroups in isoflurane-anesthetized rats using previously described classification schemes, one based on shape of the extracellularly recorded spike waveform and another based on functional connectivity of GP neurons to the cortex, and quantify changes in these groups following DA depletion.

Studies in animals anesthetized with injectable anesthetics suggest that GP neurons can be functionally classified into subtypes and each may play a unique role in PD. The inhalational anesthetic isoflurane will be used, allowing more constant and easily regulated levels of anesthesia than injectable anesthetics. GP neurons in rats will be studied electrophysiologically, to determine if previously described functional classifications of GP neurons may be confirmed, and if they display different responses to dopamine depletion.

Specific Aim 2:

Test the hypothesis that low doses of raclopride selectively block DA autoreceptors and potentiate the therapeutic effect of L-DOPA on behavior.

DA autoreceptors are DA receptors on DA neurons, consisting exclusively of D2-like receptors. Activation of DA autoreceptors inhibits DA cell firing and reduces DA release. Raclopride, a selective D2 antagonist, is known to block the autoreceptor–mediated negative-feedback inhibition of DA neurons, thereby increasing DA release in the striatum. Previous results have shown that DA autoreceptors are extremely sensitive to DA agonists such as apomorphine; at low doses, apomorphine activates DA autoreceptors without affecting DA receptors post-synaptic to DA terminals [23, 95].

Our hypothesis is that DA autoreceptors are also more sensitive than DA postsynaptic receptors to D2 antagonists such as raclopride. Behavioral tests will be conducted to investigate whether co-administration of a low dose of raclopride enhances the therapeutic effect of L-DOPA. Low doses of raclopride (2.5, 5, or 10 μg/kg) will be co-administered with L-DOPA (6 mg/kg) to determine whether they can block the inhibitory effect of L-DOPA on DA neurons and enhance the therapeutic effect of L-DOPA in Parkinsonian animals (6-OHDA lesioned rats).

CHAPTER TWO

RAT GLOBUS PALLIDUS NEURONS: FUNCTIONAL CLASSIFICATION AND EFFECTS OF DOPAMINE DEPLETION

Brad Karain[1], Dan Xu[2], John A. Bellone[3], Richard E. Hartman[3], Wei-Xing Shi[1,2]

Departments of Basic Sciences[1], Pharmaceutical Sciences[2], and Psychology[3]

Loma Linda University Schools of Medicine, Pharmacy, and Behavioral Health

Loma Linda, CA 92350, USA

To be Published: Movement Disorders

Abstract

Background: The rat globus pallidus is homologous to the primate globus pallidus externus. Studies of rats anesthetized with injectable anesthetics suggest that pallidal neurons can be functionally classified into subtypes (I and II) based on spike shape, and that each plays a unique role in Parkinson's disease. In this study, we examined the electrophysiology of pallidal neurons using the inhalational anesthetic isoflurane, which offers more constant and easily regulated levels of anesthesia than injectable anesthetics. We also tested whether subtypes of pallidal neurons respond differently to dopamine depletion. **Methods**: Pallidal neurons were recorded extracellularly in isoflurane-anesthetized rats. Cortical local field potentials were simultaneously recorded to determine the functional connectivity of individual neurons to the cortex. **Results**: All pallidal neurons fired Type-II spikes when recorded with small tip, high-impedance electrodes. Type-I spike shapes were observed only with large tip, low-impedance electrodes. Pallidal neurons can also be classified as positively coupled, negatively coupled, or uncoupled according to their functional connectivity to the cortex. All three types were found under isoflurane anesthesia. Lesions of dopamine neurons using 6-hydroxydopamine decreased uncoupled cells, increased negatively coupled cells, and altered the phase relationship of positively coupled cells to the cortex. **Conclusions**: Spike shape depends critically on the recording electrode and is not reliable in distinguishing Type-I and Type-II neurons. Positively coupled, negatively coupled, and uncoupled cells are found in isoflurane-anesthetized rats and are differentially affected by dopamine depletion.

Abbreviations

PC: positively coupled

NC: negatively coupled

UC: uncoupled

DA: dopamine

6-OHDA: 6-hydroxydopamine

GP: globus pallidus

Introduction

The rat globus pallidus (GP) is homologous to the human external GP. Based on extracellularly recorded spike shape, two types of GP neurons have been previously reported, Type-I and Type-II [20, 50]. Type-I spikes have a negative initial phase, whereas Type-II spikes have a positive initial phase. Under ketamine anesthesia, the two types were reported to be in equal abundance, but Type-I neurons had a faster axonal conduction velocity and were inhibited, instead of being excited, by the dopamine (DA) agonist apomorphine [20]. GP neurons can also be classified based on their functional connectivity to the cortex. Positively coupled (PC) or Type-Active neurons fire during the active phase of cortical slow oscillation (SO), whereas negatively coupled (NC) or Type-Inactive cells fire during the inactive phase of the SO [9, 69, 70]. Neurons whose firing shows no correlation with cortical activity are referred to as uncoupled cells (UC). Recently, NC neurons are shown to innervate primarily downstream basal ganglia nuclei such as the subthalamic nucleus, while PC cells project heavily back to the striatum [22].

In this study, we asked whether GP neurons in isoflurane-anesthetized rats can be similarly classified. As an inhalational anesthetic, isoflurane provides more constant and easily regulated levels of anesthesia than injectable anesthetics used in previous

studies. We also asked whether DA depletion produces different effects on different types of GP neurons.

Materials and Methods

All procedures were performed in accordance with protocols approved by the Institutional Animal Care and Use Committee and in compliance with National Institutes of Health *Guide for the Care and Use of Laboratory Animals*. Male Sprague-Dawley rats (Harlan, Indianapolis, IN), weighing between 250 and 400g, were used. Unless otherwise noted, all drugs were purchased from Sigma-Aldrich (St. Louis, MO).

Electrophysiology

Rats were anesthetized with isoflurane (Butler Schein Animal health, Dublin, OH, 3.0% for surgery, maintained at 1.5%) or ketamine (150 mg/kg, i.p.). GP neurons were recorded extracellularly using techniques described previously.[96-98] Briefly, glass electrodes (World Precision Instruments, Sarasota, FL) were pulled using a PE-2 puller (Narishige, Long Island, NY) and filled with 0.5 M NaAc and 1% pontamine sky blue (Bio/Medical Specialties, Santa Monica, CA), providing an impedance of about 30 MΩ (measured in vitro using 1 kHz 100 pA current pulses). For some recordings, the electrode tip was broken back to about 2 μm and filled with 2 M NaCl or 0.5 M NaAc, providing an impedance of approximately 4 and 15 MΩ, respectively.

GP recordings were made in the right hemisphere (P 0.8-1.2, L 2.6-3.0, V 5.0-7.0 mm from bregma). Local field potentials (LFPs) were recorded with an additional electrode inserted into the motor cortex (M1: A 2.0, L 3.0, V 2.0 mm from bregma). Signals were amplified by a CyberAmp 380 (Molecular Devices, Sunnyvale, CA) and filtered online using a single pole RC filter (0.3-2 kHz for spike recording and 0.1-100 Hz for LFP recording, Clampex, Molecular Devices). Body temperature was maintained at

37±0.5°C with a homeothermic blanket system (Harvard Apparatus Inc., Holliston, MA). Following each recording session, the recording site was marked by electrophoretic ejection of pontamine sky blue through the microelectrode (-20 μA, 10 min). Recording sites were verified using standard histological techniques [99, 100].

6-Hydroxydopamine Injections

In some animals, DA neurons were lesioned by 6-hydroxydopamine (6-OHDA, 8 μg/4 μl) injected into the right medial forebrain bundle (P 4.4, L 1.2, V 7.8 mm from bregma). Thirty minutes prior to the injection, animals were pretreated with desipramine (Bio Trend, Destin, FL, 12.5 mg/kg, i.p.) to protect noradrenergic neurons. Two to three weeks after 6-OHDA treatment, apomorphine (50 μg/kg) was injected subcutaneously, and the number of contralateral rotations counted for 30 minutes. Only animals exhibiting four or more turns per minute were included as lesioned animals.

The lesion was confirmed by immunostaining for tyrosine hydroxylase. Briefly, 40 μm serial sections containing the substantia nigra were cut and incubated with 1% H_2O_2 for 20 min. Sections were washed with PBS and incubated with a blocking buffer (5% goat serum, 0.1% Triton X-100, for 1 hour at room temperature) followed by monoclonal antibody to tyrosine hydroxylase raised in rabbit (dilution 1:1000, Invitrogen, Carlsbad, CA, for 24 hours at 4°C). Tyrosine hydroxylase was visualized by incubating the sections with horseradish peroxidase-goat anti-rabbit antibody (dilution 1:2000, Invitrogen, for 2 hrs at 4°C) followed by Stable DAB (Invitrogen, for 10 minutes or until the color sufficiently darkened). DAB reaction was terminated with a final rinse in PBS.

Data Analysis

All analyses were performed using Clampfit 10 (Molecular Devices) and in-house VBA subroutines in Excel (Microsoft, Redmond, WA). Firing rate and variability of firing,

estimated by the coefficient of variation (CV) and CV2 of interspike intervals, were determined every 10 sec. CV2 is less sensitive to firing rate variations than CV [101]. Firing periodicity was analyzed using methods similar to those described previously [96-98]. Briefly, rate histograms (bin width: 10 ms) were constructed based on a 2 min stable recording selected from each cell. Following tapering using the Hanning-Tukey window function and removal of the linear trend, a fast Fourier transform (FFT) was performed to yield spectra with a resolution of 0.097 Hz. LFP autospectra (down-sampled to 100 Hz) were obtained using similar methods. The degree of correlation between GP cell firing and cortical LFP was evaluated using cross-spectral and coherence analysis. Phase lags were calculated from portions of the phase spectrum encompassing the peak frequencies of cross spectra.

Phase lags were also determined using a Hilbert transform (HT)-based method, [102] in which cortical LFPs were first band-pass filtered using a zero-phase, 12-pole Butterworth filter. After the HT, instantaneous phases corresponding to each spike were determined. The circular mean of all spike phases was then calculated and reported as the mean phase of a GP neuron relative to cortical LFP. In both the FFT and HT-based methods, the peak of the cortical up state was defined as 0°. PC neurons were defined as cells showing significant coupling to cortical LFP with a phase lag >-90° and <90°. All other coupled cells were classified as NC cells. Numerical results were expressed as mean±SEM. Phase value differences were evaluated based on the D and U2 values derived from the Kuiper's V test and the Watson U2 test, respectively. Significance of all other data was determined based on the Z values provided by the two tailed Mann-Whitney U test.

Results

Type-I and II Neurons

A total of 80 GP neurons were recorded from 48 isoflurane-anesthetized rats. All cells fired Type-II spikes (Fig. 2.1A). To test whether Type-I cells were suppressed, recordings were made from two ketamine-anesthetized rats. In a previous study using ketamine, 50% of GP neurons were Type-I and 50% Type-II [20]. In this study, all GP neurons (n=29) recorded under ketamine were still Type-II. In one cell, the spike initially presented as Type-I, but as the electrode advanced to the vicinity of the cell, the spike transitioned to Type-II (Fig. 2.1A).

To determine whether spike shape depends on the electrode used, recordings were made using electrodes similar to those used by Kelland et al. [20]. Thus, the electrode tip was broken back to about 2 μm and filled with 2 M NaCl or 0.5 M NaAc. As would be expected, the impedance of these electrodes was reduced (2 M NaCl: 3.3-4.5 MΩ, 0.5 M NaAc: 13-16 MΩ) compared to our routinely used, small tip electrodes (30-34 MΩ). Using large-tip electrodes, 72 GP cells were recorded from two isoflurane-anesthetized rats. Of these cells, 44 were Type-I, 18 Type-II, and 10 initially Type-I that then transitioned into Type-II.

Type-I cells may have a narrow initial rising phase only detectable by a high-impedance electrode. Supporting this possibility, Type-II spikes recorded with large-tip electrodes were narrower (0.24±0.01 ms, n=18) than those recorded with small tip electrodes (0.33±0.01 ms, n=80, $z=3.95$, $p<0.001$). Also consistent with this possibility, spikes recorded in ketamine-anesthetized rats using small-tip electrodes showed a bimodal distribution (Fig. 2.1B). In the single neuron that initially showed Type-I spikes and eventually displayed a positive initial peak, the half-maximal width of the initial peak was 0.27 ms, which is near the center of the smaller of the two ranges for the bimodal distribution. However, in transitional cells recorded with large-tip electrodes, the initial

positive phase was broader (0.29±0.02 ms, n=10) than that of Type-II cells (0.24±0.01 ms, n=18, $z=2.4$, $p<0.05$). Additionally, the initial rising phase was shortened under isoflurane compared to ketamine (0.41±0.02 ms, n=29, $z=3.68$, $p<0.001$, Fig. 2.1B).

Unfiltered raw recordings were compared to filtered signals to rule out the possibility that the online filter converts Type-I spikes into Type-II. Off-line filtering was also performed. None of the filters tested changed the polarity of the initial phase (Fig 2.1C).

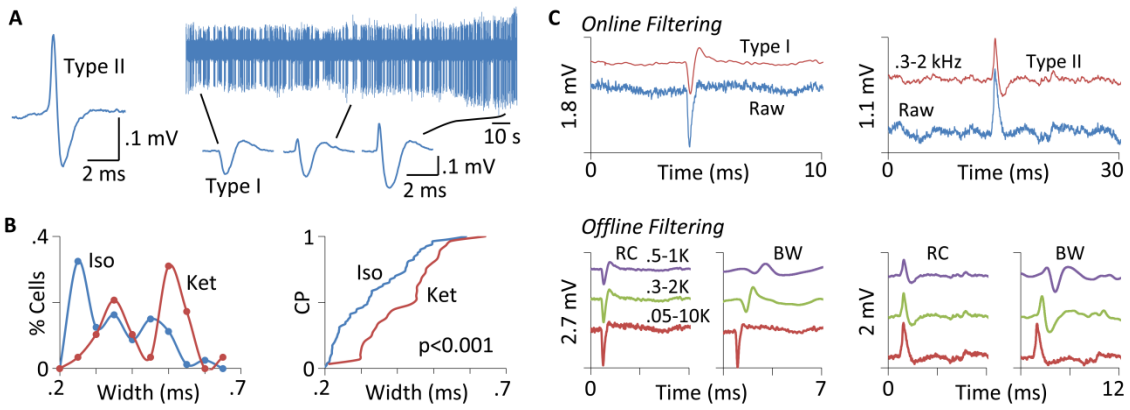

Figure 2.1 Shape of extracellularly recorded action potentials of GP neurons. **A**) Recordings showing a typical Type-II spike recorded from a GP neuron in an isoflurane-anesthetized rat (left) and the transition of spike, recorded from a GP neuron in a ketamine-anesthetized rat, from Type-I to Type-II as the electrode approached the cell (right). The leftmost action potential (Type-I) was recorded furthest from the cell. **B**) Ordinary (left) and cumulative distributions (right, CP, cumulative probability) of spike widths. Under ketamine, spike widths exhibited a bimodal distribution (red). Isoflurane significantly shifted the distribution to a narrower range (blue). **C**) Upper traces are raw (blue) and online-filtered recordings (red) of a Type-I (left) and Type-II spike (right). The online filter was a single-pole RC filter with a bandpass of 0.3-2 kHz. Lower traces are the same raw signals offline-filtered by either a single-pole RC or 12-pole Butterworth (BW) filter. Three bandpass settings (0.05-10k, 0.3-2k, and 0.5-1 kHz) were tested. None changed the polarity of the initial peak of the spike.

Positively Coupled, Negatively Coupled, and Uncoupled Pallidal Neurons

To identify PC, NC, and UC cells, dual-site recordings were made from 5 isoflurane-anesthetized rats. Fig 2.2 shows phase analysis results from a typical PC neuron. The FFT-based method suggests that at the peak frequency of the cross spectrum (0.59 Hz), cortical activity lags GP activity by 35.3°. The HT method using a bandpass filter selective for the SO (0.1-1.5 Hz) or a narrow bandpass filter (±0.4 Hz) centering at 0.59 Hz produced similar results. Fig 2.2 also shows that the phase spectrum derived from the FFT method is relatively insensitive to filtering (Fig 2.2 B-D). For simplicity, in the remainder of this paper we only report results from the HT method using a bandpass filter of 0.1-1.5 Hz.

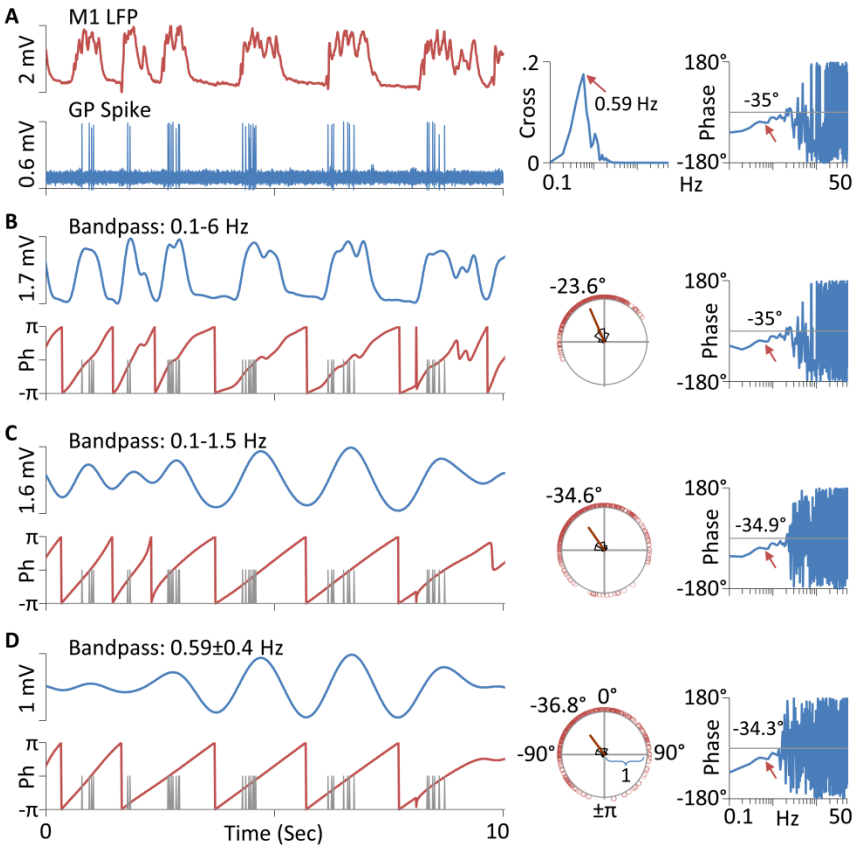

Figure 2.2 Comparison of FFT and HT-based phase analysis. **A**) Left traces are segments of recordings of LFPs in the primary motor cortex (M1 LFP, red) and spike activity of a GP neuron (GP Spike, blue) in an isoflurane-anesthetized rat. Right charts are the cross and phase spectrum of the two recordings showing that at the peak frequency of the cross spectrum (0.59 Hz), cortical activity lagged behind the activity of the GP neuron by 35.3°. **B-D**) Shown on the left are the same LFPs but filtered by three different bandpass filters (blue), corresponding instantaneous phases derived from the HT of filtered LFPs (red, y-axis ranging from -180° to 180°), and GP spike times (gray). On the right are circular plots of instantaneous phases corresponding to all spikes recorded from the GP neuron (red circles) and phase spectra obtained from FFT analysis of filtered LFPs. Included also in the circular plot are the circular histogram (binwidth: 30°, black) and the mean vector (circular mean of all spike phases, red line). The length of the mean vector ranges from 0 to 1 and indicates the dispersion of spike phases. The low and high-cutoff frequencies of the three bandpass filters were 0.1-6 Hz (B), 0.1-1.5 Hz (C), and 0.59±0.4 Hz (D), respectively. The circular mean varied from -23.6° to -36.8° depending on the filter used. In contrast, the phase value, measured at 0.59 Hz by the FFT method, was virtually unchanged by filtering.

In 40 GP neurons recorded, 16 (40%) were identified as PC cells, 7 (17.5%) NC cells, and 17 (42.5%) UC cells (Fig 2.3A). These neurons differred not only in functional connectivity, but also firing rate. NC cells fired significantly faster than PC ($z=3.14$, $p<0.005$) and UC cells ($z=2.57$, $p=0.01$). They also showed reduced CV2 compared to PC ($z=3.21$, $p<0.005$) and UC cells ($z=2.25$, $p<0.05$)(Fig 2.3B). A comparison of firing rate with previous studies is complicated by the fact that often only GP neurons firing between 10 and 70 Hz were studied [34, 39]. Since both PC and UC cells were found to fire considerably slower than 10 Hz, the possibility exists that PC and UC cells were unintentionally excluded from analysis in those earlier studies. Also, those earlier studies used rats anesthetized with chloral hydrate, or awake rats paralyzed with gallium triethiodide.

Since choice of anesthetic is known to have large effects on neuronal activity in the GP (neurons in rats anesthetized with urethane fire at half the rate of GP neurons in rats paralyzed with gallamine triethiodide [58]), the results we report using isoflurane-anesthetized rats are unsurprisingly quite different from reported rates in earlier studies. A similar problem occurs for classification of GP neurons by functional connectivity with cortical neurons as PC, NC, or UC. Earlier studies used urethane-anesthetized rats [69] and found 75% of GP neurons to fire in 'direct phase' with cortical activity (PC cells). Other studies used urethane supplemented with ketamine/xylazine and found 75% of GP neurons in control rats to be UC cells, with 10% NC and 15% PC. GP neurons in lesion rats were found to be 72% NC, 17% PC and 12% UC [70]. Our results differ in that we find roughly equal numbers of UC and PC cells, although our results agree with these previous studies concerning lesion rats where instead of large numbers of UC cells we instead find many more NC cells and fewer UC cells with only small changes in the number of PC cells.

Dual-site recordings were also made in one ketamine-anesthetized rat, in which 6/12 GP neurons were identified as PC, 1 NC, and 5 UC. Under ketamine, UC cells (0.11±0.03 spikes/sec) fired slower than PC cells (16.44±11.04, $z=2.74$, $p<0.01$). Their firing rate was also slower than that of UC cells under isoflurane (6.71±2.75, $n=17$, $z=2.15$, $p<0.05$).

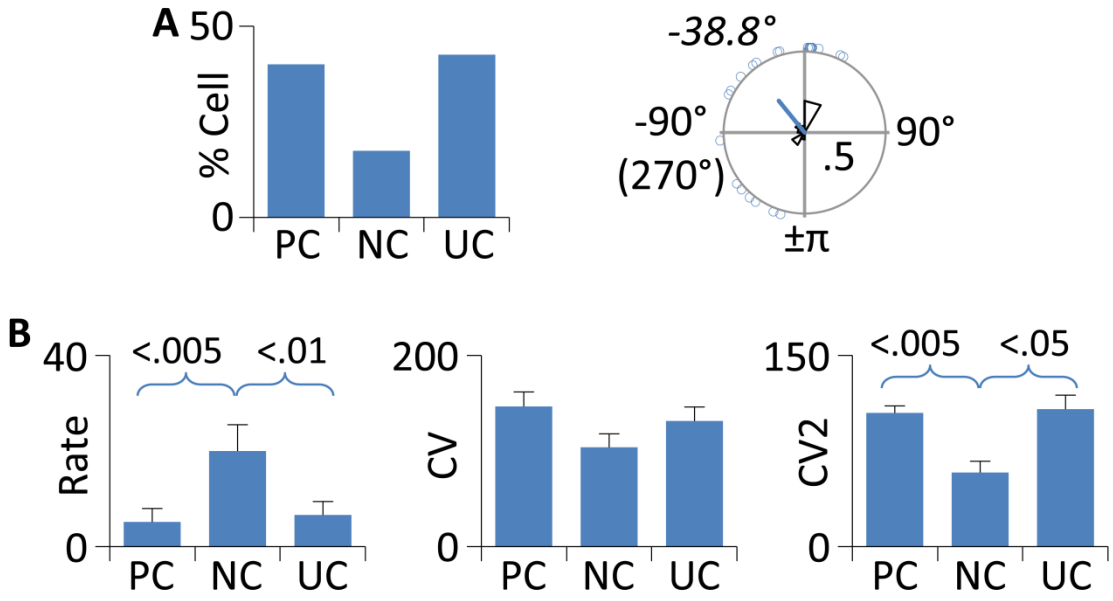

Figure 2.3 GP neurons in isoflurane-anesthetized rats. **A**) Bar graph showing distribution of PC, NC, and UC cells in isoflurane-anesthetized rats (left) and circular plot of mean phases of all GP neurons showing functional coupling to the cortex. Of all GP cells recorded, 40% were PC cells, 17.5% NC cells, and 42.5% UC cells. Included also in the circular plot are the circular histogram (black) and the mean vector (blue line). **B**) Bar graphs comparing firing rate, CV and CV2 between subtypes of GP neurons. NC cells fired significantly faster and had a reduced CV2 compared to both PC and UC cells.

Effects of 6-OHDA Lesions

In six 6-OHDA-lesioned, isoflurane-anesthetized rats, 52 GP neurons were recorded, of which 22 (42.3%) were PC cells, 19 (36.5%) NC cells, and 11 (21.2%) UC cells. Compared to controls, lesions of DA neurons decreased UC cells from 42.5% to 21.2% and increased NC and PC cells from 17.5% to 36.5% and 40% to 42.3%, respectively. In each subgroup, DA depletion had no effect on firing rate, CV, and CV2, except an increase in CV in PC cells ($n1=22$, $n2=16$, $z=2.28$, $p<0.05$, Fig 2.4).

Lesions of DA neurons significantly changed phases of GP neurons ($d=0.487$, $p<0.001$, $u2=0.21$, $p<0.05$, Fig 2.4A). Further analysis suggests that the change is due to a shift in phase in PC cells ($d=0.585$, $p<0.005$, $u2=0.203$, $p<0.05$, Fig 2.4).

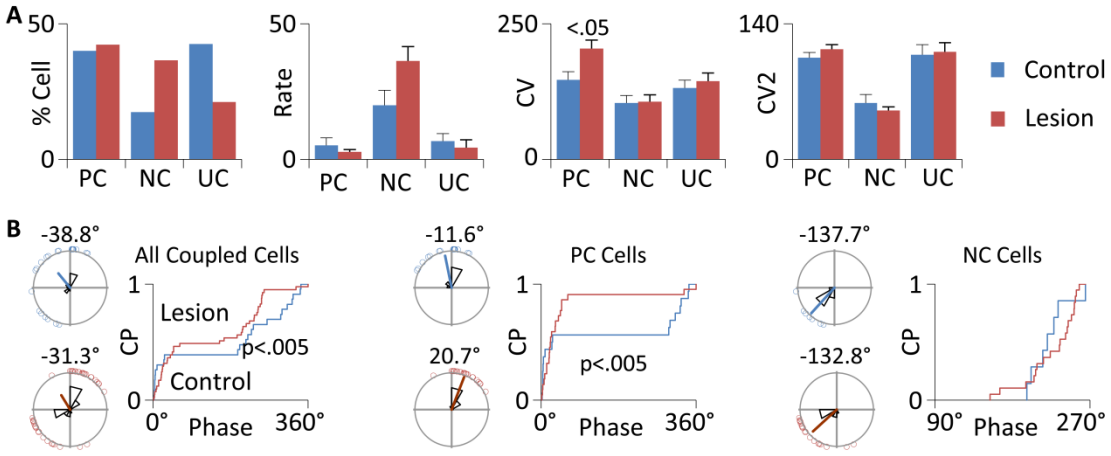

Figure 2.4 Effects of 6-OHDA lesions on GP neurons. **A**) Bar graphs comparing proportions of PC, NC, and UC cells, and their firing rate , CV and CV2 in control (blue) and 6-OHDA lesioned rats (red, Lesion). Lesions of DA neurons increased PC and NC cells and decreased UC cells. Except an increase in CV in PC neurons, the lesions had no effect on firing rate, CV, and CV2 of the three subtypes of GP neurons. **B**) Circular plots and cumulative distributions of phases of all coupled cells (left), PC cells (center), and NC cells (right). Compared to controls (blue), a significant shift in phase was observed in GP neurons recorded in 6-OHDA lesioned rats (red). When PC and NC neurons were analyzed separately, a significant change was observed only in PC cells and not in NC cells. In control rats, cortical activity lagged the activity of PC cells by an average of 11.6°. In lesioned rats, cortical activity led the activity of PC cells by 20.7°.

Discussion

This study showed that all GP neurons fired Type-II spikes when recorded with small-tip electrodes of high impedance. Type-I neurons were observed only with large-tip electrodes. PC, NC, and UC neurons were present in isoflurane-anesthetized rats, differed significantly in firing rate and regularity, and were differentially affected by lesions of DA neurons.

Type-I and Type-II GP Neurons

Earlier studies found two types of striatal neurons based on the spike shape, Type-I and Type-II [23]. Studies in the GP observed similar waveforms and used the same designations [20, 29, 34, 35, 50, 53]. In this study, all GP neurons recorded with small-tip electrodes fired Type-II spikes. Our evidence further suggests that Type-II spikes may exhibit as Type-I when recorded with large-tip electrodes. Consistent with this suggestion, the initial positivity of Type-II waveforms diminishes when low-impedance electrodes are used [103], and only Type-I spikes are observed when tungsten electrodes are used [54, 78].

Type-I and Type-II cells also differ in axonal conduction velocity and response to the DA agonist apomorphine [20]. While our recordings do not allow classification based on polarity of the initial spike phase, recordings in ketamine-anesthetized rats suggest that cells with a narrow initial phase may be Type-I and those with a broad initial phase may be Type-II since the initial peak widths are bimodally distributed. In the single cell that transitioned from Type-I to Type-II, the initial peak width was near the center of the smaller of the two ranges in the bimodal distribution. However, recordings using large-tip electrodes suggest the opposite. Thus, in these recordings, the initial positive peak of transitional cells, which might be Type-I, was significantly wider than that of cells initially presenting as Type-II. We also found that spike width varied depending on the electrode

used. Type-II spikes recorded with small-tip electrodes were significantly wider than those recorded with large-tip electrodes. Taken together, these results suggest that when recorded extracellularly, neither spike polarity nor spike width is reliable in distinguishing Type-I from Type-II GP neurons.

Positively Coupled, Negatively Coupled, and Uncoupled Neurons

Phase lag between GP and cortical activity was determined using both FFT and HT methods. The latter has the advantage of being applicable to nonstationary signals and maintaining information in the time domain. The technique, however, requires filtering to extract signals of specific frequencies. We found that narrow-band filters centering at the peak frequency of the cross-spectrum (±0.1 to ±0.5 Hz) or covering the entire range of the SO (0.1-1.5 Hz) produced results similar to those derived from the FFT method. For simplicity, this study only reports results obtained using a bandpass filter of 0.1-1.5 Hz.

This study showed that under isoflurane anesthesia, 40% of GP neurons recorded were PC cells, 17.5% NC cells, and 42.5% UC cells. These numbers differ from those reported previously. In one study, 91% GP cells recorded in ketamine-anesthetized rats were functionally coupled to cortical activity, while under urethane most GP cells were uncoupled [9]. In another study also using urethane, 72% of GP neurons were PC and 2% NC [69]. In a study using urethane supplemented with ketamine, only 15% were PC and 10% NC [70]. The discrepancy may have been caused by multiple factors including differences in anesthesia, data analysis, and electrode. Low-impedance electrodes have been suggested to preferentially record NC cells [22].

We found that PC, NC, and UC cells also differed significantly in firing rate and regularity. NC cells fired significantly faster and showed a reduced firing variability

compared to PC and UC cells. These results raise the possibility that NC cells correspond to high frequency, low CV pausers (HFP) found in the primate external GP, whereas PC and/or UC cells correspond to low frequency, high CV bursters (LFB) [77, 78]. However, differences in species and use of anesthesia require further investigation to test this possibility. One study suggests that rat GP neurons can be similarly classified as HFP and LFB, but the two groups of cells show no difference in firing rate in rats [78].

PC and NC neurons have been recently shown to project to different basal ganglia nuclei [22]. Their difference in functional connectivity suggests that they also receive different inputs. For example, the cortex may modulate PC cells through subthalamic glutamate neurons and NC cells through striatal GABA neurons [3, 104, 105]. Two observations suggest that this scheme is overly simplified. First, NC cells fired significantly faster than PC cells, suggesting that they also receive an excitatory input and/or PC cells are tonically influenced by an inhibitory input. Second, cortical activity lagged behind GP activity in many cells (see circular histograms in Figs 3 and 4), suggesting that oscillatory activities in these cells are not driven solely by the cortex, but in conjunction with other areas. For example, the thalamus, known to trigger cortical SO [106], provides extensive glutamate projections to the striatum and subthalamic nucleus [3, 107, 108]. A direct innervation of the GP by the thalamus has also been demonstrated [107]. Thus, the anatomical basis underlying the differences in functional connectivity between PC, NC, and UC neurons remains to be determined.

Effects of 6-OHDA lesions

Lesions of DA neurons induced by 6-OHDA produced two main effects on GP neurons. First, the lesions increased PC cells from 40% to 42.3% and NC cells from 17.5% to 36.5%, but decreased UC cells from 42.5 to 21.2%. Qualitatively similar

results were observed in a previous study using urethane supplemented with ketamine, in which 6-OHDA lesions increased PC cells from 15% to 17% and NC cells from 10% to 72% [70]. However, in another study also using urethane, 6-OHDA lesions decreased PC neurons from 72% to about 30%, increased NC cells from about 2% to 43%, and slightly increased UC cells [69]. The cause for the discrepancy is unknown and may be related to the differences in type and level of anesthesia as well as electrodes used in different studies. As mentioned earlier, low-impedance electrodes may preferentially record NC cells [22].

The second main effect of 6-OHDA lesions observed in this study was the phase change in PC cells. Under control conditions, cortical activity led GP activity in about 56% of PC cells (Fig 2.4). Following 6-OHDA lesions, cortical activity led GP activity in 91% of PC cells. Interestingly, the lesions only slightly increased the number of PC cells. In contrast, lesions of DA neurons significantly increased the number of NC cells but had no significant effect on their phases. If the STN and Str are partially responsible for the functional coupling between PC and NC cells to the cortex, respectively, our results would suggest that lesions of DA neurons alter information transmission through both nuclei.

To summarize, Type-I and Type-II GP neurons, while likely representing distinct neuronal populations, are poorly represented by the spike shape, even though this is how they were originally defined. PC, NC, and UC cells are present in isoflurane-anesthetized rats. The three subtypes of GP neurons differ from each other not only in functional connectivity to the cortex, but also in firing rate, firing regularity, and responses to lesions of DA neurons. These results support the suggestion that the three subtypes of GP neurons play different roles in PD.

CHAPTER THREE

POTENTIATION OF L-DOPA'S EFFECT ON BEHAVIOR

Abstract

Previous studies have shown that asymmetrical forelimb use during exploration in the cylinder test is highly sensitive to levels of dopamine (DA) depletion and to the therapeutic effect of antiparkinsonian drugs [109]. Using the test, daily L-DOPA administration (6 mg/kg) has been shown to be behaviorally effective for up to 140 minutes with substantial abnormal involuntary movements (AIMs) appearing within 3 weeks of repeated administration [110]. AIMs are unwanted side effects caused by chronic use of L-DOPA. We hypothesize that co-administration of a small dose of a D2 antagonist potentiates the antiparkinsonian effect of L-DOPA so that lower doses of L-DOPA can be used to reduce or to delay AIMs. The goal of this study is to use the cylinder test to determine whether raclopride at behaviorally ineffective doses (2.5, 5, or 10 μg/kg) blocks L-DOPA induced inhibition of DA neurons and whether at those doses it enhances L-DOPA's therapeutic effect.

Our results suggest that at 5 μg/kg (i.v.), raclopride can significantly potentiate the therapeutic effect of L-DOPA in a subgroup of animals. A more sensitive test with an improved signal-to-noise ratio could provide a more confident answer regarding significance.

Abbreviations

DA: Dopamine

6-OHDA: 6-hydroxydopamine

D3: dose of L-DOPA (3 mg/kg)

R2.5/5/10: dose of raclopride (2.5, 5, or 10 μg/kg)

Introduction

Investigations in rodents of skilled forepaw actions, including placing, grooming, or foot faults, have clear correlates in Parkinson's disease, and are, therefore, the most sensitive ways of detecting motor impairment following dopamine loss from the basal ganglia of rodents. The rotarod and cylinder test were found to reveal significant motor impairment in lesioned animals, but only the cylinder test revealed improvement due to dopaminergic drugs [90]. Developing and using tests that have the ability to identify behavioral deficits is essential to expanding the development of translational therapies. The cylinder test, a modification of a test first described in 1990 [91] has been found to have the ability to detect even mild neurological impairments [92]. Chemical toxins capable of producing degeneration of the nigrostriatal dopaminergic pathway are commonly used in animal models of PD in both rodents and primates, contributing significantly towards the development of symptomatic therapies for PD patients. Translational success depends upon an accurate assessment of these models. A sensitive test should evaluate the degree of impairment, any neuroprotection afforded, and any therapeutic improvement due to treatment [111].

Kirik et al. induced partial lesions of the nigrostriatal dopamine system using the neurotoxin 6-OHDA. A differential sensitivity was found regarding the degree of damage to the nigrostriatal pathway, depending on which behavioral test was used. A 60-70% reduction in tyrosine hydroxylase (TH)-positive fiber density in the lateral striatum, accompanied by a 50-60% reduction in TH-positive cells in substantia nigra (SN), is sufficient for the induction of significant impairment in the stepping test. Impaired skilled paw-use, on the other hand, was obtained only with a four-site (4 x 7 microgram) lesion, which induced 80-95% reduction in TH fiber density throughout the rostrocaudal extent of the lateral striatum and a 75% loss of TH-positive neurons in SN [112]. The cylinder test is sensitive to lesions as small as 30% [109], and is able to measure recovery of

sensorimotor function independent of the extent of test experience. The cylinder test is sensitive to dopaminergic neurodegeneration of the nigrostriatal system [113], and may be used with animals not naive to the test [111].

Our preliminary electrophysiological data suggests that at behaviorally ineffective low doses (10 μg/kg or less), raclopride significantly reduces or blocks L-DOPA induced inhibition of DA neurons. Fig. 3.1 shows two firing traces of a DA neuron in the SNc of a healthy rat. The top trace shows a DA neuron firing at ~8 Hz that drops to ~5 Hz after i.v. administration of L-DOPA (50 mg/kg, i.v.). The bottom trace shows an initial injection of raclopride (20 μg/kg. i.v.) completely blocks a subsequent injection of L-DOPA (50 mg/kg, i.v.).

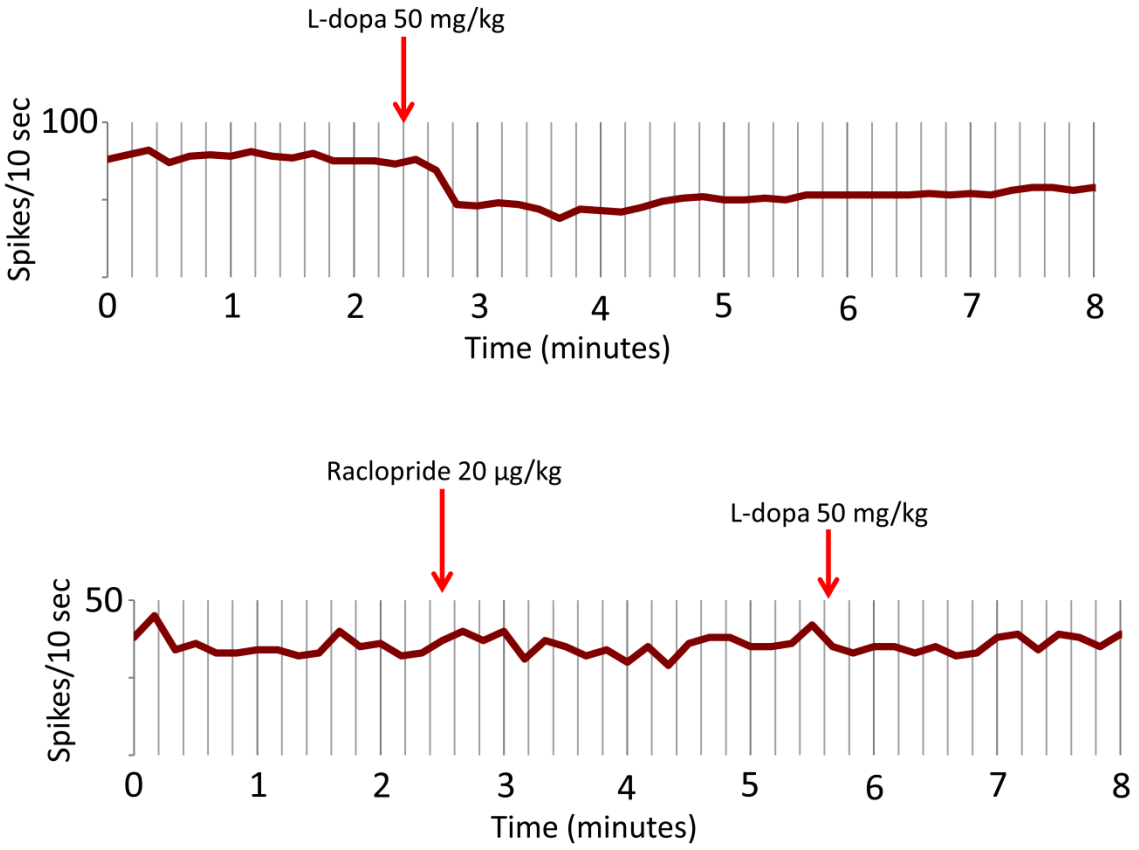

Figure 3.1 Raclopride blocks L-DOPA induced inhibition of DA neurons

Top trace shows that a DA neuron decreases its firing rate from ~8 Hz to ~5 Hz after i.v. administration of L-DOPA (50 mg/kg, i.v.). The bottom trace shows an initial injection of raclopride (20 µg/kg. i.v.) completely blocks a subsequent injection of L-DOPA (50 mg/kg, i.v.).

Thus, we hypothesize that a low dose of raclopride may selectively block DA autoreceptors and potentiate the therapeutic effect of L-DOPA on behavior. The goal of the study is to use the cylinder test to measure the deficit in movement incurred through unilateral 6-OHDA lesions of DA neurons and to test whether raclopride co-administered with L-DOPA enhances L-DOPA's therapeutic effect.

Materials and Methods

All procedures were performed in accordance with protocols approved by the Institutional Animal Care and Use Committee and in compliance with National Institutes of Health *Guide for the Care and Use of Laboratory Animals*. Male Sprague-Dawley rats (Harlan, Indianapolis, IN), weighing between 250 and 400g, were used. Unless otherwise noted, all drugs were purchased from Sigma-Aldrich (St. Louis, MO).

Partial Lesion Model

Rats were rendered unconscious with 3.0% isoflurane (maintained at 2.0% at start of injection) and mounted in a stereotaxic apparatus. Animals received three unilateral stereotaxic injections of 6-OHDA (7 µl) in the right striatum. The injection was made at a rate of 1.0 µl/min using a 0.1 mm cannula connected by polyethylene tubing to a 10µl Hamilton microsyringe driven by an infusion pump (Stoelting). The syringe needle was left in place after each injection for an additional 2 minutes, then withdrawn slowly to prevent reflux of the solution. The 7 µl doses were administered at the striatal coordinates, measured in mm relative to Bregma, (AP, ML, DV): (+1.0,-3.0,-5.0), (-0.1,-3.7,-5.0), (-1.2,-4.5,-5.0). To minimize variability due to degradation of the toxin, 6-OHDA solutions were freshly made with ice-cold saline containing 0.03% ascorbic acid, kept on ice and protected from exposure to light [112]. While desipramine is normally administered 30 minutes prior to 6-OHDA injections to protect norepinephrine terminals,

it has not been demonstrated to be required in this model as no neurons other than nigral DA neurons have been shown to be harmed by 6-OHDA injections in these striatal regions.

Cylinder Test

This test is a modification of the forelimb asymmetry motor test first described by Schallert and Lindner [91], was performed as described by Kirik et al. [111]. Briefly, the animal is placed in a clear glass cylinder approximately 20 cm diameter x 30 cm height. The animal is allowed to move freely for 5 minutes while being visually recorded. Mirrors are placed behind the cylinder so that the video camera has visual access to all paw placements around the cylinder. The data are presented as impaired (contralateral) forepaw contacts as a percentage of the total forepaw contacts. Recorded time points were 50, 100, 150, 200, and 250 minutes following the single-injection drug administration (i.p.)

Results

Model Verification

Immunofluorescence staining is shown for animal A38 (Fig. 3.3) for histological verification of the results from the cylinder test. Fig. 3.2 shows a coronal brain slice through the SNc, immunostained for tyrosine hydroxylase (TH). While TH is not exclusive to DA neurons, TH is a marker exclusive to DA neurons in the region shown. Notice that the unilateral 6-OHDA injections into the right Str caused a marked reduction in DA neurons on the ipsilateral (right) side. This is in agreement with the degree of reduction seen in % left paw use for animal A38 in Fig. 3.3.

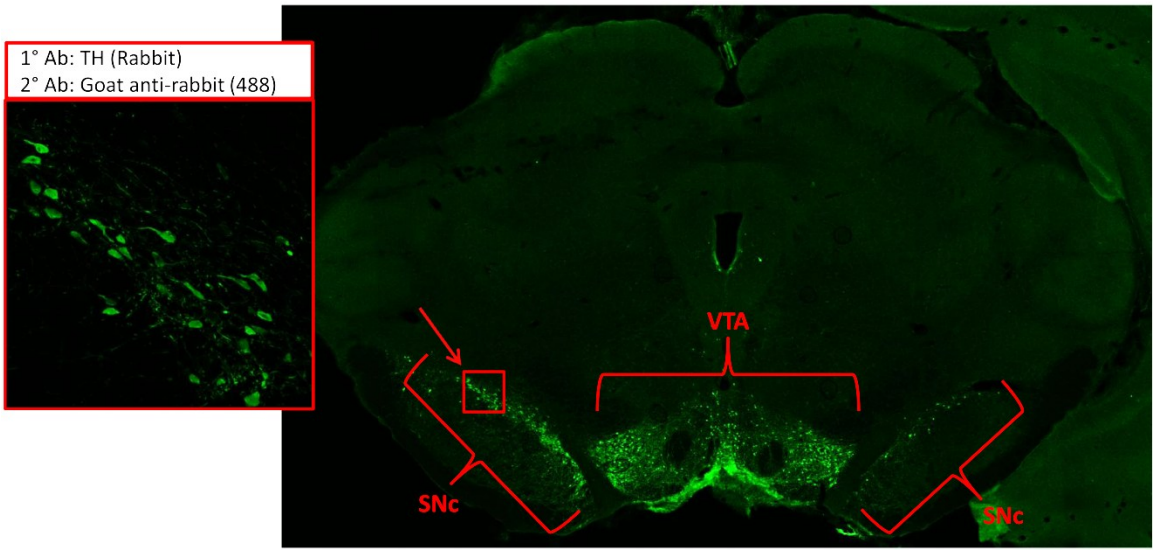

Figure 3.2 TH immunostaining for coronal section through SNc and VTA in rat brain showing lesions of DA neurons by 6-OHDA injection in the striatum. A decrease in TH+ cell bodies is seen on the lesioned (right) side of the brain in the SNc. As expected, this lesion model does not diminish DA cell bodies in the VTA.

Sensitivity of Cylinder Test

Fig. 3.3 shows the activity of rats in the cylinder test, both as healthy animals (pre-lesion) and as parkinsonian animals (post-lesion). The top diagram shows the % Left Paw Use for each animal both before and after 6-OHDA lesion. The left paw is the impaired paw for animals with a unilateral lesion on the right side of the brain. The solid blue bar illustrates that each animal experiences ~50% use of the left paw before 6-OHDA was administered unilaterally to lesion DA neurons in the right Str (axons) and SNc (cell bodies). The solid red bar illustrates the use of the left paw two weeks following the lesion (6-OHDA) surgery. This demonstrates that the cylinder test quite easily detects the difference between healthy (control) animals and parkinsonian (6-OHDA lesion) animals.

The middle diagram shows the total touches on the wall surface completed with the either paw (# with right paw + # with left paw + (# with both paws simultaneously x 2)). The solid blue bar indicates how many touches were completed in a test session prior to lesion surgery, while the solid red bar shows the total touches completed two weeks following surgery. As expected, animals are generally much more active before surgery than after.

Animals A27 through A38 were used only for preliminary data, with animal A41 excluded due to insufficient movement during testing. Notice in particular animal A27, which shows no deficit due to the lesion surgery. Any animal showing a similar lack of deficit would not have been included in the study. Interestingly, while A27 shows no deficit of left paw use due to 6-OHDA lesion, there is a marked reduction in total activity (from 34 touches to 13). This suggests that the surgery itself may cause a significant reduction in the activity of the animal recorded in the cylinder two weeks after the surgery.

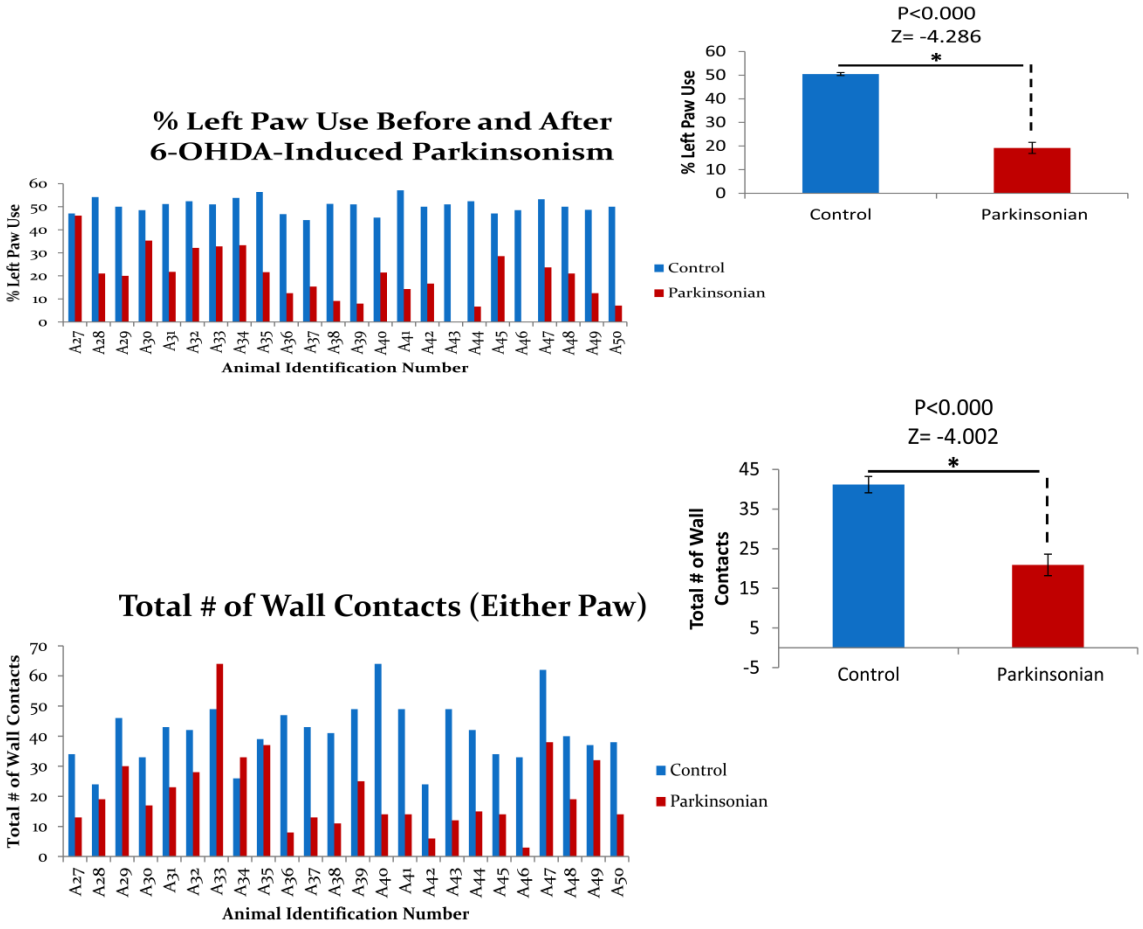

Figure 3.3 Cylinder test before and after 6-OHDA lesion. Top figure shows the cylinder test is very sensitive to 6-OHDA lesions. All 24 rats but two showed a clear decrease in left paw use after the lesion. The bottom figure shows that the same animals were generally much less active in the cylinder test following surgery (parkinsonian) than before surgery (control). Insets for each figure show the means for each diagram with significant decrease in % Left Paw Use ($p<0.001$) and significant decrease in Total # of Wall Contacts ($p<0.001$) respectively.

Fig 3.4 shows correlation analysis for Fig 3.3. The leftmost diagram shows there is no correlation between total activity and use of the left paw (before surgery when the animals were healthy). The center diagram shows a very weak correlation between total activity and % use of the left paw in the same animals following lesion induction (when the animals were parkinsonian). The rightmost diagram is a correlation analysis between the change in total activity (from control to parkinsonian) versus the change in % use of the left paw (from control to parkinsonian), and shows a very weak correlation. These results suggest that the decrease in left paw use in lesioned rats is not secondary to the decrease in total activity.

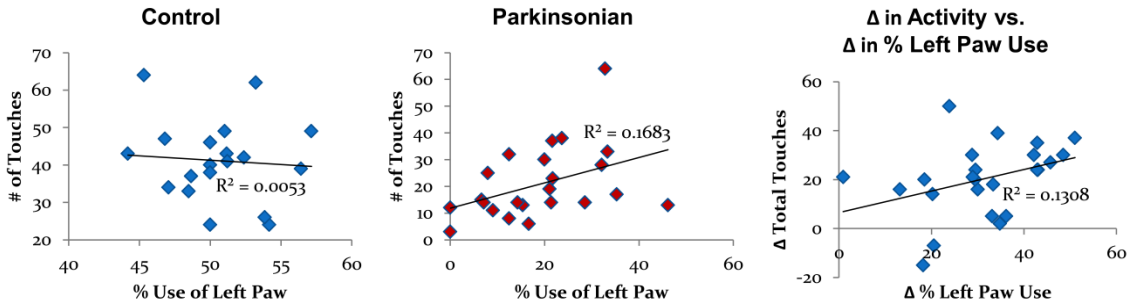

Figure 3.4 Correlation of Activity with Left Paw Use. The leftmost diagram shows there is no correlation between total activity and use of the left paw (before surgery when the animals were healthy). The center diagram shows a very weak correlation between total activity and % use of the left paw in the same animals following lesion induction (when the animals were parkinsonian). The rightmost diagram is a correlation analysis between the change in total activity (from control to parkinsonian) versus the change in % use of the left paw (from control to parkinsonian), and shows a very weak correlation.

Consistency of Cylinder Test

The cylinder test is most often used at a single time point post following lesion induction. Thus there remains some uncertainty as to consistency of the results when the animal is well-habituated to the cylinder. One of the ways to measure potentiation of the therapeutic effect of L-DOPA is to determine if the therapeutic effect lasts longer. Therefore, the modified treatment is to be measured not simply at a single time point, but at several consecutive time points. We found that the subject was most active when initially introduced to the cylinder, but while the activity level subsequently declined, the decline was asymptotic instead of linear.

Fig.3.4 shows the total activity level of 11 animals given only a saline injection, calculated as the total number of times either the left or right forepaw touched the cylinder while the rear paws supported a rearing posture. The activity at the initial time point (50 min) was normalized to 100%, and the activity at subsequent time points is shown as a percentage of this value, diminishing from 100% at the first time point (50 min) to approximately 70% at the final two time points (200 min and 250 min). That the final value is approached asymptotically rather than linearly suggests the animal would perform adequately even if further time points were attempted. Importantly, the number of times the impaired paw was used relative to the total number of wall touches remained relatively constant, from 14.9% +/- 2.7% (50 min) to 15.6% +/- 3.8% (250 min).

These results show for the first time that the % use of the impaired paw (contralateral to lesion side of the brain) is independent of the total activity level and are consistent with data shown in fig 3.3 which shows no correlation between total activity and % use of the left paw in healthy (control) animals, and only a very weak correlation in 6-OHDA lesion (parkinsonian) animals. Fig. 3.3 also shows a similarly very weak correlation between the change in activity due to lesion and % use of the left paw.

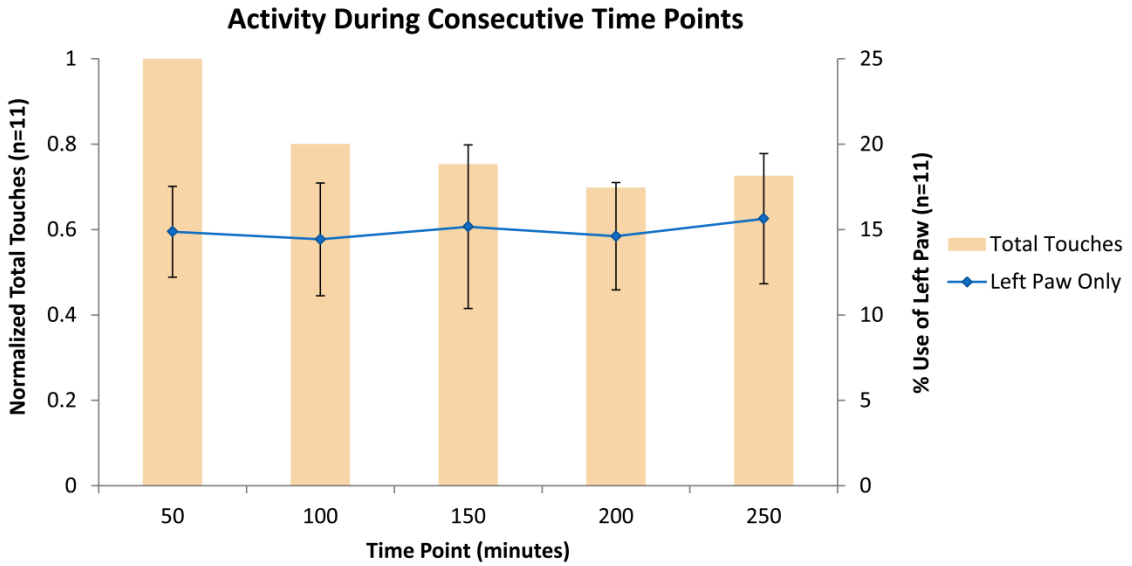

Figure 3.5 Cylinder Test at Consecutive Time Points. Bars show the Total activity levels at different time points (normalized to 100% at the first time point, 50 min, as this is the event with highest activity). Subsequent time points (100 min, 150 min, 200 min, and 250 min) are seen to decrease non-linearly to about 70% for the measurements at 200 and 250 min, quantified using the vertical axis on the left. The percentage of time that the impaired paw is used is shown by the blue diamonds, quantified by the vertical axis on the right. Use of the left paw (as a percentage) does not appear to depend on overall activity level, ranging from 14.9% +/- 2.7% (50 min) to 15.6% +/- 3.8% (250 min).

Correcting for Different Sets of Model Animals

Many factors may confound the behavioral results of the cylinder test. Lesion size and location will be the largest variables, but these in turn depend on factors which in theory are identical but in practice will have slight variations, such as effectiveness of the lesioning neurotoxin 6-OHDA. For instance, the 6-OHDA was made fresh every 3 hours, kept in the dark and on ice. However, since the surgical groups were on different days, small variations in concentration or effectiveness could have been introduced. For this reason the % use of the left (impaired) paw was tracked during vehicle injection for 4 consecutive weeks, starting at 3 weeks post-lesion. Figure 3.5 shows group 2 (n=6) has an improvement in left paw use over the four weeks that was larger than the improvement shown by group 1 (n=5). Improvement in ability to use the impaired paw was unexpected, as it is generally presumed that the lesions are progressive and permanent.

The possibility exists that the neuronal axons and cell bodies may well be perishing in a progressive and permanent manner, but the animal is nevertheless adapting to the disability in such a way that an overall improvement in behavioral score is observed. Another possibility is that the improved movement score seen in succeeding weeks is partly due to a long-term benefit of the injection of L-DOPA from the previous week. One possibility for the differential recovery rate observed between groups 1 and 2 could be that the group 2 animals received smaller lesions (on average) and therefore recovered faster (on average) than the animals in group 1. Schallert et al. showed that performance in the cylinder test, as a function of dopamine depletion was significant ($r=0.91$, $p<0.001$) [113]. The correlation between SN DA cell loss and cylinder test performance in mice is not as strong [114].

This is important for interpreting the dose-response curve (Fig. 3.6), because a moving baseline will artificially inflate the apparent therapeutic benefit of raclopride co-

administered with L-DOPA. Achieving an accurate dose response curve requires adjusting the cylinder test scores according to the weekly baseline measurements. The slope of the line for each group was used to adjust behavioral scores of later weeks for comparison to the baseline values obtained in the first week.

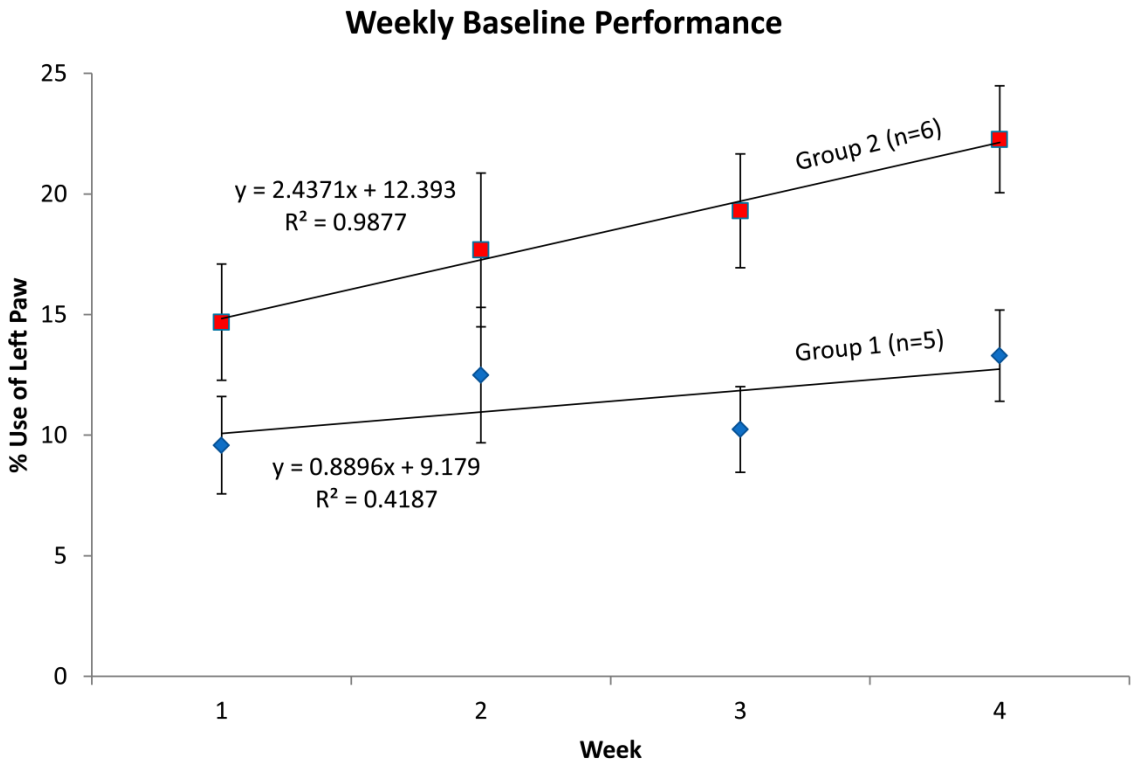

Figure 3.6 Spontaneous behavioral recovery of separate surgical groups. Lesions were induced through stereotactic surgery in two groups of animals on two consecutive days. Group 2 (n=6) has an improvement over the four weeks of testing that was larger than the improvement shown by group 1 (n=5).

Dose Response

If raclopride does indeed potentiate the therapeutic value of L-DOPA, the possibility exists that there may be an optimum dose, above and below which efficacy is diminished. Fig. 3.6 shows the dose response for L-DOPA (3 mg/kg) being co-administered with raclopride (0 μg/kg, 2.5 μg/kg, 5 μg/kg, and 10 μg/kg), broken down to show each time point.

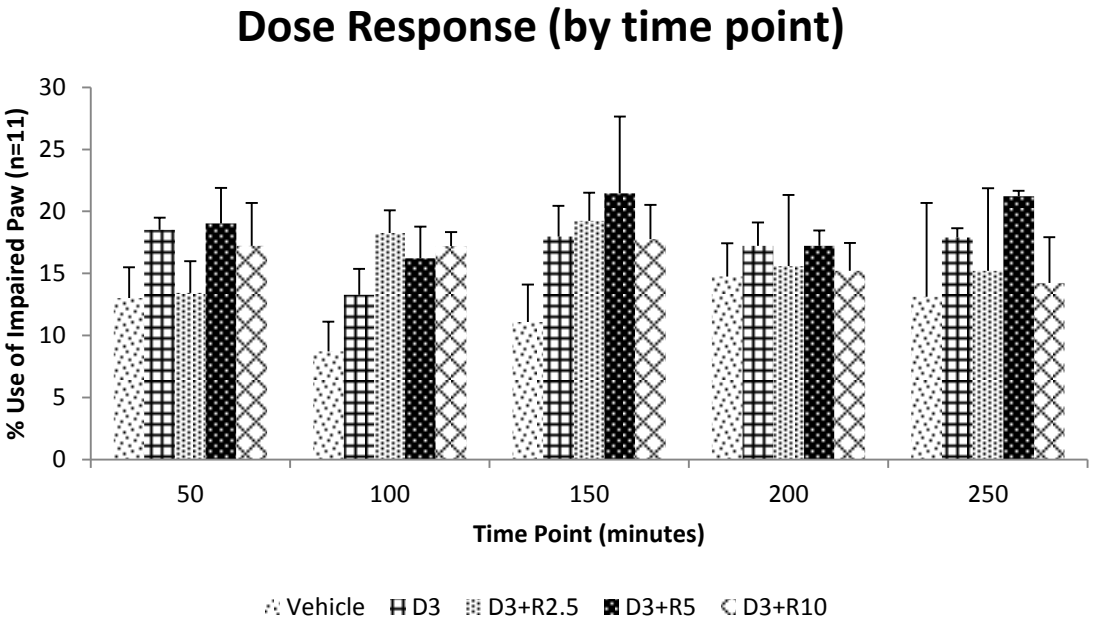

Figure 3.7 Dose response across all time points. The dose response for L-DOPA (3 mg/kg) being co-administered with raclopride (0, 2.5, 5 and 10 µg/kg) for 50, 100, 150, 200, and 250 minutes.

Since no particular time point stands out, the time points are averaged and displayed in Fig. 3.7. Interestingly, while there is an improvement over vehicle in each case where L-DOPA was administered, the only raclopride dose showing some improvement over L-DOPA alone was the 5 μg/kg dose. All treatments were significantly improved over vehicle (saline) with p and z values of (0.029, -2.179) (0.033,-2.131) (0.001,-3.181) and (0.028, -2.200) for saline compared to D3, D3+R2.5, D3+R5, and D3+R10 respectively. However, no statistical difference was seen between D3, D3+R2.5, D3+R5, and D3+R10. D3+R5 had the largest mean, even though not significantly different from the others, so it was the dose used for further tests.

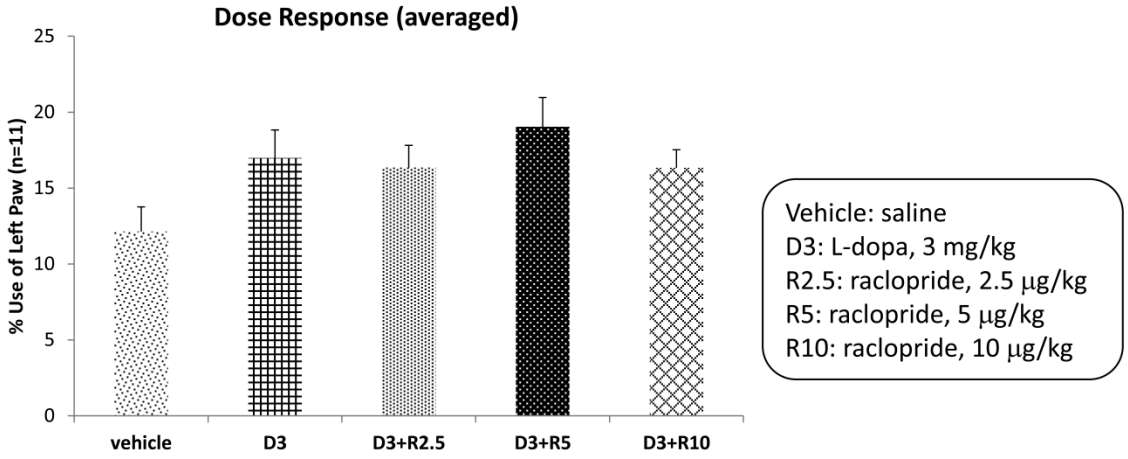

Figure 3.8 Dose Response of L-DOPA and raclopride co-administration The dose response for L-DOPA (D3, 3 mg/kg) being co-administered with raclopride at various doses: 0 (vehicle or D3), R2.5 (2.5 μg/kg), R5 (5 μg/kg), and R10 (10 μg/kg). All treatments were significantly improved over vehicle (saline) with p and z values of (0.029, -2.179) (0.033,-2.131) (0.001,-3.181) and (0.028, -2.200) for saline compared to D3, D3+R2.5, D3+R5, and D3+R10 respectively. However, no statistical difference was seen between D3 and any dose of raclopride co-administered with L-DOPA.

Therapeutic Effect of Raclopride

To avoid the possible confounding variable of a treatment injection affecting the results of another treatment injection in a later week, observations are restricted to only the first week of treatment. Fig 3.8 shows two traces, each evaluated at five time points: 50, 100, 150, 200, and 250 minutes. The top trace (n=6 animals) evaluates ability to use the left paw following administration of either saline or L-DOPA (3 mg/kg). No statistically significant improvement is observed.

The bottom trace (n=5 animals) also evaluates ability to use the left paw, but following administration of either saline or L-DOPA (3 mg/kg) co-administered with raclopride (5 μg/kg). Statistically significant improvements are observed at both 50 ($p=0.043$) and 150 ($p=0.043$) minutes, with power analysis (GPower 3.1.7) suggesting significance may be found with one additional animal ($\beta= 0.3$) at 250 minutes.

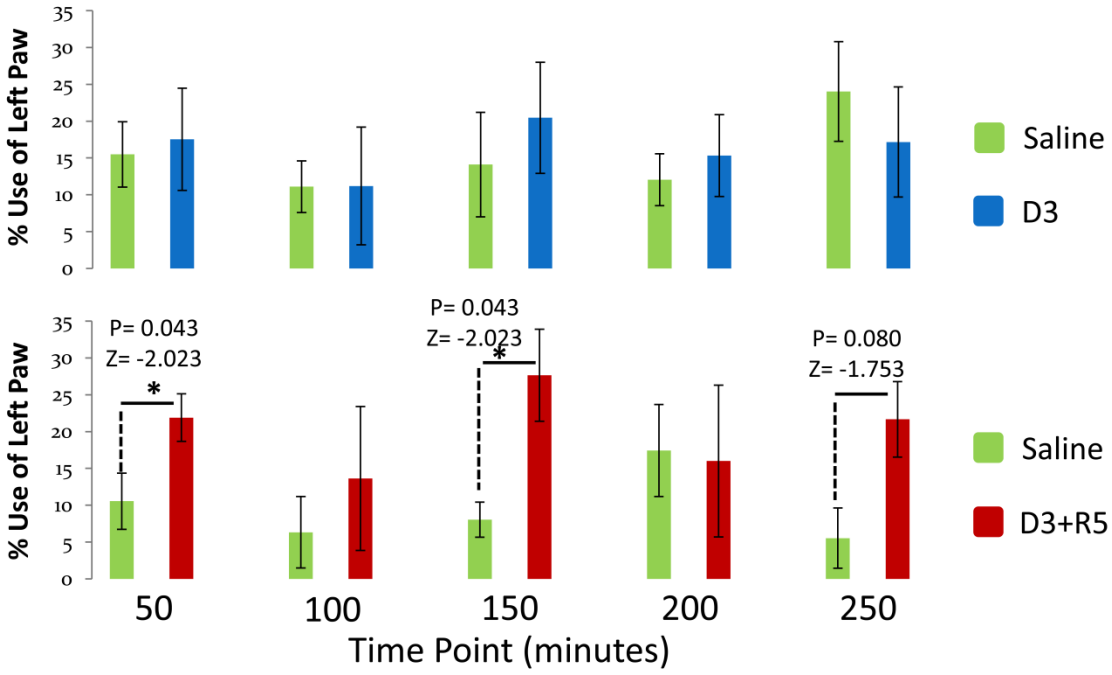

Figure 3.9 Therapeutic Effect of raclopride

Top trace (n=6 animals) evaluates ability to use the left paw at several time points (50, 100, 150, 200, 250 minutes) following administration of either saline or L-DOPA (3 mg/kg). No statistically significant improvement is observed.

Bottom trace (n=5 animals) evaluates ability to use the left paw at the same time points, but following administration of either saline or L-DOPA (3 mg/kg) co-administered with raclopride (5 µg/kg). Statistically significant improvements are observed at both 50 and 150 minutes, with power analysis (GPower 3.1.7) suggesting significance may be found with one additional animal (β= 0.3) at 250 minutes.

Overall Therapeutic Effect of Raclopride

Fig. 3.9 shows the data from Fig. 3.8, but with all time points combined. The data from each individual animal is shown in between the means of the saline and treatment groups. The graph on the left shows a comparison of % left paw use following injection of either saline or L-DOPA (3 mg/kg). No statistically significant improvement is observed from the L-DOPA injection, at any time point.

However, the graph on the right shows a similar comparison of % left paw use following injection of either saline or L-DOPA (3 mg/kg) co-administered with raclopride (5 μg/kg). A statistically significant 2-fold improvement is observed for treatment with L-DOPA combined with raclopride ($p=0.001$) compared to animals that received only saline.

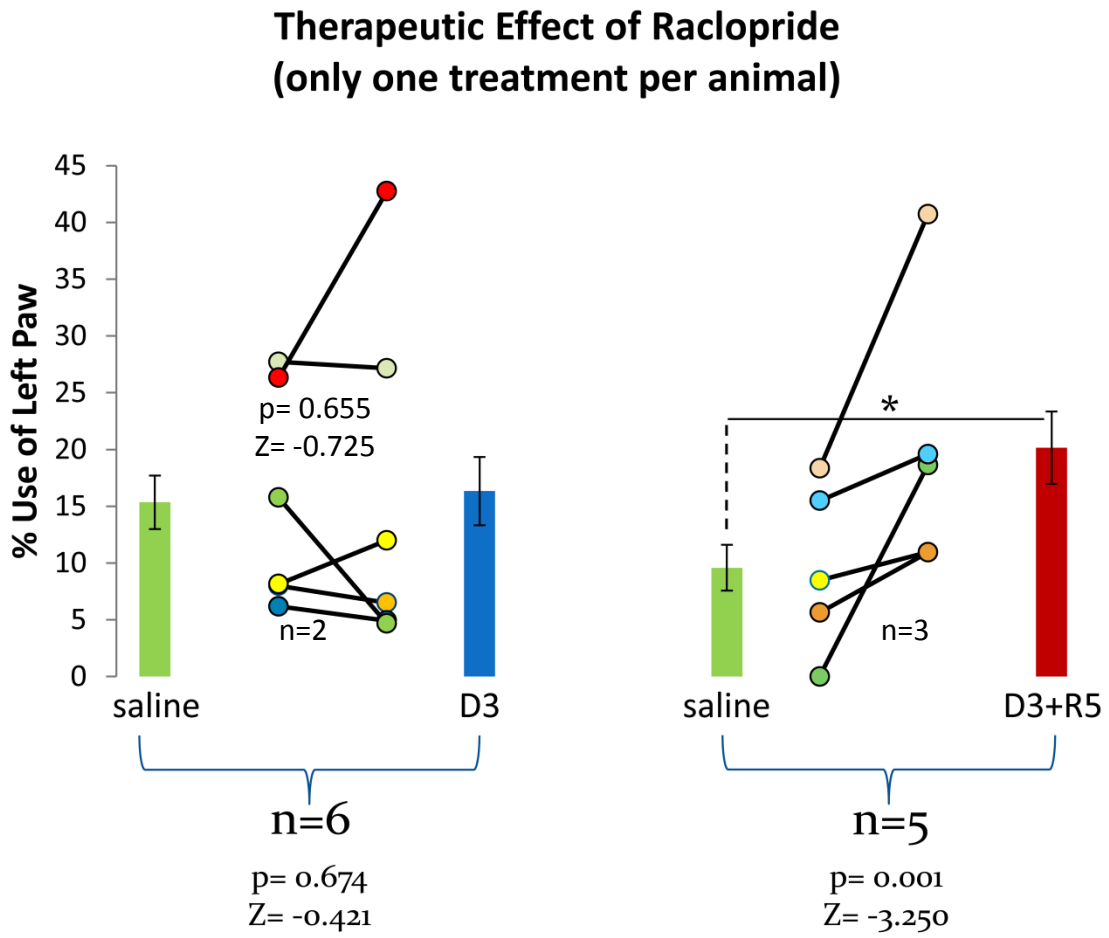

Figure 3.10 Overall therapeutic effect of raclopride. With all time points combined, the data from each individual animal is shown in between the means of the saline and treatment groups. The graph on the left (n=6 animals) shows a comparison of % left paw use following injection of either saline or L-DOPA (3 mg/kg). No statistically significant improvement is observed from the L-DOPA injection, at any time point. However, the graph on the right (n=5 animals) shows a similar comparison of % left paw use following injection of either saline or L-DOPA (3 mg/kg) co-administered with raclopride (5 µg/kg). A statistically significant 2-fold improvement is observed for treatment with L-DOPA combined with raclopride (p=0.001)

Discussion

The data is highly variable. There may be several ways to mitigate this. First, animals could be selected with similar post-surgery baseline behavioral scores. Clinically this would be similar to selecting patients with similar levels of disease progression. The possibility exists that individuals with similar levels of neurological damage could respond similarly to treatment, and that there may be a correlation with level of neurological damage and the dosage observed to be effective. All animals showed behavioral scores in the cylinder test that indicated the % left paw use (as parkinsonian animals) was independent of total activity level.

The possibility also exists of dividing model animals into two groups, those expressing many autoreceptors per DA neuron and those expressing relatively few. This selection could be performed with a straightforward behavioral test. The animals with more autoreceptors would be expected to have improved use of the impaired forelimb compared to the animals with fewer autoreceptors.

Finally, there is some uncertainty in whether the animal has actually made contact with the cylinder surface. A way may be found to measure actual rather than perceived contact. Other metrics for wall contact may prove more useful than the standard counting of ipsilateral, contralateral, or simultaneous paw placement. For instance, measuring the total time the left (or right) paw is in contact with the cylinder wall during the course of the recording period holds potential to be a more sensitive measure of impairment. A more sensitive measure could also involve a combination of total time of contact, height at which the paw touches the wall, and percentage of the paw surface which makes contact.

The critical consideration in this set of experiments is potentiation of the therapeutic benefit of L-DOPA. The dose of 3 mg/kg was specifically chosen because 6 mg/kg was found in the literature to be the smallest dose with any therapeutic benefit, as

well as the smallest dose which produced AIM's (the behavioral dyskinesias resulting from repeated long-term use of L-DOPA).

We found that raclopride (5 μg/kg) co-administered with L-DOPA (3 mg/kg) does significantly improve the therapeutic benefit of L-DOPA behaviorally, using the cylinder test for evaluation. When broken down into individual time points, statistically significant improvements were noticed at both 50 ($p=0.043$) and 150 minutes ($p=0.043$), with power analysis (GPower 3.1.7) suggesting significance may be found with one additional animal ($\beta= 0.3$) at 250 minutes.

CHAPTER FOUR

DISCUSSION AND CONCLUSION

Introduction

The hallmark pathogenic feature of Parkinson's Disease (PD) is the death of dopamine (DA) producing neurons in the substantia nigra (SN), which in a healthy subject release DA into the striatum (Str). The most effective treatment is an orally administered drug, L-DOPA, a DA precursor permeable to the blood-brain barrier. As a DA precursor, L-DOPA acts to re-establish reduced striatal DA levels. However, long-term use of L-DOPA results in dose-dependent side effects which are at least as debilitating as the disease itself.

Hypothesis

In this thesis we hypothesize that a low dose of raclopride (a D2 antagonist) selectively blocks DA autoreceptor-mediated feedback inhibition of DA neurons, thereby potentiating L-DOPA's effects on neurons postsynaptic to DA terminals including GP neurons. To test this hypothesis we employed both electrophysiology and behavioral tests. Preliminary data suggested that doses of raclopride as low as 10 ug/kg may block the DA autoreceptor -mediated inhibition of DA neurons induced by L-DOPA. Raclopride is not currently known to have any other biological effect at this dose, and therefore should have no effect on post-synaptic receptors.

Electrophysiological Studies

In the course of the electrophysiological studies it was realized that the method demonstrated in previous studies for identifying distinct subgroups of GP neurons was

actually incorrect. Previous studies used a method which looked at the shape of the extracellularly recorded action potential, dividing these into Type-I with a negative initial peak, and Type-II with a positive initial peak. We found that Type-I and Type-II waveforms are due to electrode tip-size and impedance, rather than the action potential itself. Thus, an alternative method was used, in which subgroups of GP neurons were identified by functional connectivity (UC, PC, or NC) with cortical neurons. We found that UC, PC, and NC neurons in the GP also differed significantly in firing rate and pattern in a manner not entirely consistent with previous studies, suggesting that differences in anesthesia and electrode type may be of greater importance than heretofore acknowledged. Following 6-OHDA lesions, the number of NC cells increased with no change in phase relationship to cortical activity. Before 6-OHDA lesions ~50% of PC cells in the GP are seen to lag cortical activity, but following 6-OHDA lesions cortical activity leads GP activity in ~91% of PC cells in the GP. Since there are no direct cortical projections to GP neurons, the phase shift of PC cells is likely to be due to the influence of STN neurons with synaptic connections to GP neurons. The drop in UC cells, with concomitant increase in NC cells, might be due to increased cortico-GP coupling through Str after 6-OHDA lesions. These results lay the basis for future studies to investigate the effect of L-DOPA combined with raclopride on GP neurons.

Behavioral Studies

For behavioral studies, we decided to use L-DOPA at 3 mg/kg, just below the threshold known to have therapeutic benefit, in combination with raclopride at 5 ug/kg (a dose not known to have any biological effect) in order to test the potentiation of L-DOPA's therapeutic benefit.

Potentiation of the therapeutic benefit of L-DOPA by a small dose of raclopride may occur in several ways. First, the effect of treatment may be more pronounced. Second the effect of treatment may last longer. Third, the treatment may delay the onset

of the dyskinesias evident with long-term repeated use of L-DOPA. Behaviorally, the most effective dose of raclopride to potentiate the therapeutic effect of L-DOPA was 5 μg/kg. A small increase or decrease in dose led to behavioral scores in the cylinder test which not only had no statistically significant difference from the scores obtained from administering L-DOPA alone, but whose means were actually below that of L-DOPA alone. This suggests that those doses are at best not efficacious, and at worst injurious. However, importantly, all treatments in the dose response curve (Fig. 3.7) were significantly improved over saline. This implies that other doses of raclopride may have been equally efficacious.

We found that the degree of behavioral impairment is independent of the overall activity level. Also, the degree of behavioral impairment was observed to decrease from week to week. The possibility exists that behavioral scores in successive weeks were affected by treatment injections from previous weeks. Another possibility is that the animals were recovering due to an adaptation that worked to counteract the behavioral deficit the animal faced. Receptor sensitization also may have been occurring, which would similarly explain the spontaneous recovery in behavioral scores.

Conclusion

We found that raclopride (5 μg/kg) co-administered with L-DOPA (3 mg/kg) does significantly improve the therapeutic benefit of L-DOPA behaviorally. However, we recommend further study to confirm the optimum combinatory dose for L-DOPA and raclopride. The possibility exists that the 2-fold increase in therapeutic benefit already observed could be increased further yet. In terms of human studies, considering the effect on DA autoreceptors requires still living DA neurons, it would be advantageous to introduce subjects to the therapy as early as possible.

REFERENCES

1. Smith, Y., et al., Microcircuitry of the direct and indirect pathways of the basal ganglia. Neuroscience, 1998. 86(2): p. 353-87.

2. Redgrave, P., et al., Goal-directed and habitual control in the basal ganglia: implications for Parkinson's disease. Nat Rev Neurosci, 2010. 11(11): p. 760-72.

3. Lanciego, J.L., N. Luquin, and J.A. Obeso, Functional neuroanatomy of the Basal Ganglia. Cold Spring Harb Perspect Med, 2012. 2(12).

4. Kita, H., Globus pallidus external segment. Prog Brain Res, 2007. 160: p. 111-33.

5. Oviedo, A., A. Delgado, and E. Querejeta, Differential inhibition of globus pallidus neurons by electrical or chemical stimulation of the striatum. Neurosci Res, 2008. 62(4): p. 240-5.

6. Sadek, A.R., P.J. Magill, and J.P. Bolam, A single-cell analysis of intrinsic connectivity in the rat globus pallidus. J Neurosci, 2007. 27(24): p. 6352-62.

7. Kita, H. and S.T. Kitai, Intracellular study of rat globus pallidus neurons: membrane properties and responses to neostriatal, subthalamic and nigral stimulation. Brain Res, 1991. 564(2): p. 296-305.

8. Ni, Z., et al., Changes in the firing pattern of globus pallidus neurons after the degeneration of nigrostriatal pathway are mediated by the subthalamic nucleus in the rat. Eur J Neurosci, 2000. 12(12): p. 4338-44.

9. Magill, P.J., J.P. Bolam, and M.D. Bevan, Relationship of activity in the subthalamic nucleus-globus pallidus network to cortical electroencephalogram. J Neurosci, 2000. 20(2): p. 820-33.

10. Goldberg, J.A., S.S. Kats, and D. Jaeger, Globus pallidus discharge is coincident with striatal activity during global slow wave activity in the rat. J Neurosci, 2003. 23(31): p. 10058-63.

11. Hassani, O.K., M. Mouroux, and J. Feger, Increased subthalamic neuronal activity after nigral dopaminergic lesion independent of disinhibition via the globus pallidus. Neuroscience, 1996. 72(1): p. 105-15.

12. Wilson, C.J. and M.D. Bevan, Intrinsic dynamics and synaptic inputs control the activity patterns of subthalamic nucleus neurons in health and in Parkinson's disease. Neuroscience, 2011. 198: p. 54-68.

13. Breit, S., et al., Effects of 6-hydroxydopamine-induced severe or partial lesion of the nigrostriatal pathway on the neuronal activity of pallido-subthalamic network in the rat. Exp Neurol, 2007. 205(1): p. 36-47.

14. Kita, H. and T. Kita, Role of Striatum in the Pause and Burst Generation in the Globus Pallidus of 6-OHDA-Treated Rats. Front Syst Neurosci, 2011. 5: p. 42.

15. Walters, J.R., et al., Phase relationships support a role for coordinated activity in the indirect pathway in organizing slow oscillations in basal ganglia output after loss of dopamine. Neuroscience, 2007. 144(2): p. 762-76.

16. Burkhardt, J.M., et al., Synchronous oscillations and phase reorganization in the basal ganglia during akinesia induced by high-dose haloperidol. Eur J Neurosci, 2007. 26(7): p. 1912-24.

17. Nambu, A. and R. Llinas, Electrophysiology of globus pallidus neurons in vitro. J Neurophysiol, 1994. 72(3): p. 1127-39.

18. Nambu, A. and R. Llinas, Morphology of globus pallidus neurons: its correlation with electrophysiology in guinea pig brain slices. J Comp Neurol, 1997. 377(1): p. 85-94.

19. Cooper, A.J. and I.M. Stanford, Electrophysiological and morphological characteristics of three subtypes of rat globus pallidus neurone in vitro. J Physiol, 2000. 527 Pt 2: p. 291-304.

20. Kelland, M.D., et al., In vivo characterization of two cell types in the rat globus pallidus which have opposite responses to dopamine receptor stimulation: comparison of electrophysiological properties and responses to apomorphine, dizocilpine, and ketamine anesthesia. Synapse, 1995. 20(4): p. 338-50.

21. Cruz, A.V., et al., Effects of dopamine depletion on information flow between the subthalamic nucleus and external globus pallidus. J Neurophysiol, 2011. 106(4): p. 2012-23.

22. Mallet, N., et al., Dichotomous organization of the external globus pallidus. Neuron, 2012. 74(6): p. 1075-86.

23. Skirboll, L.R., A.A. Grace, and B.S. Bunney, Dopamine auto- and postsynaptic receptors: electrophysiological evidence for differential sensitivity to dopamine agonists. Science, 1979. 206(4414): p. 80-2.

24. Ruskin, D.N., et al., Drugs used in the treatment of attention-deficit/hyperactivity disorder affect postsynaptic firing rate and oscillation without preferential dopamine autoreceptor action. Biol Psychiatry, 2001. 49(4): p. 340-50.

25. Kohler, C., et al., Specific in vitro and in vivo binding of 3H-raclopride. A potent substituted benzamide drug with high affinity for dopamine D-2 receptors in the rat brain. Biochem Pharmacol, 1985. 34(13): p. 2251-9.

26. Ogren, S.O., et al., The selective dopamine D2 receptor antagonist raclopride discriminates between dopamine-mediated motor functions. Psychopharmacology (Berl), 1986. 90(3): p. 287-94.

27. Hall, H., et al., Animal pharmacology of raclopride, a selective dopamine D2 antagonist. Psychopharmacol Ser, 1989. 7: p. 123-30.

28. Ericson, H., et al., Effects of intermittent and continuous subchronic administration of raclopride on motor activity, dopamine turnover and receptor occupancy in the rat. Pharmacol Toxicol, 1996. 79(6): p. 277-86.

29. Walters, J.R., et al., D1 dopamine receptor activation required for postsynaptic expression of D2 agonist effects. Science, 1987. 236(4802): p. 719-22.

30. Hooper, K.C., et al., Quinpirole inhibits striatal and excites pallidal neurons in freely moving rats. Neurosci Lett, 1997. 237(2-3): p. 69-72.

31. Bergstrom, D.A. and J.R. Walters, Dopamine attenuates the effects of GABA on single unit activity in the globus pallidus. Brain Res, 1984. 310(1): p. 23-33.

32. Cooper, A.J. and I.M. Stanford, Dopamine D2 receptor mediated presynaptic inhibition of striatopallidal GABA(A) IPSCs in vitro. Neuropharmacology, 2001. 41(1): p. 62-71.

33. Ruskin, D.N., et al., Cocaine or selective block of dopamine transporters influences multisecond oscillations in firing rate in the globus pallidus. Neuropsychopharmacology, 2001. 25(1): p. 28-40.

34. Bergstrom, D.A., S.D. Bromley, and J.R. Walters, Dopamine agonists increase pallidal unit activity: attenuation by agonist pretreatment and anesthesia. Eur J Pharmacol, 1984. 100(1): p. 3-12.

35. Bergstrom, D.A., S.D. Bromley, and J.R. Walters, Apomorphine increases the activity of rat globus pallidus neurons. Brain Res, 1982. 238(1): p. 266-71.

36. Bergstrom, D.A. and J.R. Walters, Neuronal responses of the globus pallidus to systemic administration of d-amphetamine: investigation of the involvement of dopamine, norepinephrine, and serotonin. J Neurosci, 1981. 1(3): p. 292-9.

37. Bergstrom, D.A., S.D. Bromley, and J.R. Walters, Time schedule of apomorphine administration determines the degree of globus pallidus excitation. Eur J Pharmacol, 1982. 78(2): p. 245-8.

38. Carlson, J.H., D.A. Bergstrom, and J.R. Walters, Neurophysiological evidence that D-1 dopamine receptor blockade attenuates postsynaptic but not autoreceptor-mediated effects of dopamine agonists. Eur J Pharmacol, 1986. 123(2): p. 237-51.

39. Carlson, J.H., D.A. Bergstrom, and J.R. Walters, Stimulation of both D1 and D2 dopamine receptors appears necessary for full expression of postsynaptic effects of dopamine agonists: a neurophysiological study. Brain Res, 1987. 400(2): p. 205-18.

40. Carlson, J.H., et al., Acute reduction of dopamine levels alters responses of basal ganglia neurons to selective D-1 and D-2 dopamine receptor stimulation. Eur J Pharmacol, 1988. 152(3): p. 289-300.

41. Qi, R. and L. Chen, Different effects of dopamine D1 receptor on the firing of globus pallidus neurons in rats. Neurosci Lett, 2011. 488(2): p. 164-7.

42. Carlson, J.H., et al., Nigrostriatal lesion alters neurophysiological responses to selective and nonselective D-1 and D-2 dopamine agonists in rat globus pallidus. Synapse, 1990. 5(2): p. 83-93.

43. Burkhardt, J.M., X. Jin, and R.M. Costa, Dissociable effects of dopamine on neuronal firing rate and synchrony in the dorsal striatum. Front Integr Neurosci, 2009. 3: p. 28.

44. Soltis, R.P., et al., A role for non-NMDA excitatory amino acid receptors in regulating the basal activity of rat globus pallidus neurons and their activation by the subthalamic nucleus. Brain Res, 1994. 666(1): p. 21-30.

45. Stefani, A., et al., D2-mediated modulation of N-type calcium currents in rat globus pallidus neurons following dopamine denervation. Eur J Neurosci, 2002. 15(5): p. 815-25.

46. Ruskin, D.N., et al., Correlated multisecond oscillations in firing rate in the basal ganglia: modulation by dopamine and the subthalamic nucleus. Neuroscience, 2003. 117(2): p. 427-38.

47. Ruskin, D.N., S.S. Rawji, and J.R. Walters, Effects of full D1 dopamine receptor agonists on firing rates in the globus pallidus and substantia nigra pars compacta in vivo: tests for D1 receptor selectivity and comparisons to the partial agonist SKF 38393. J Pharmacol Exp Ther, 1998. 286(1): p. 272-81.

48. Grace, A.A. and B.S. Bunney, Paradoxical GABA excitation of nigral dopaminergic cells: indirect mediation through reticulata inhibitory neurons. Eur J Pharmacol, 1979. 59(3-4): p. 211-8.

49. Celada, P., C.A. Paladini, and J.M. Tepper, GABAergic control of rat substantia nigra dopaminergic neurons: role of globus pallidus and substantia nigra pars reticulata. Neuroscience, 1999. 89(3): p. 813-25.

50. Napier, T.C., P.E. Simson, and B.S. Givens, Dopamine electrophysiology of ventral pallidal/substantia innominata neurons: comparison with the dorsal globus pallidus. J Pharmacol Exp Ther, 1991. 258(1): p. 249-62.

51. Kelland, M.D., Sr. and J.R. Walters, Apomorphine-induced changes in striatal and pallidal neuronal activity are modified by NMDA and muscarinic receptor blockade. Life Sci, 1992. 50(22): p. PL179-84.

52. Pan, H.S. and J.R. Walters, Unilateral lesion of the nigrostriatal pathway decreases the firing rate and alters the firing pattern of globus pallidus neurons in the rat. Synapse, 1988. 2(6): p. 650-6.

53. Pan, H.S., et al., The effects of striatal lesion on turning behavior and globus pallidus single unit response to dopamine agonist administration. Life Sci, 1990. 46(1): p. 73-80.

54. Toan, D.L. and W. Schultz, Responses of rat pallidum cells to cortex stimulation and effects of altered dopaminergic activity. Neuroscience, 1985. 15(3): p. 683-94.

55. Ruskin, D.N., D.A. Bergstrom, and J.R. Walters, Multisecond oscillations in firing rate in the globus pallidus: synergistic modulation by D1 and D2 dopamine receptors. J Pharmacol Exp Ther, 1999. 290(3): p. 1493-501.

56. Bouali-Benazzouz, R., et al., Intrapallidal injection of 6-hydroxydopamine induced changes in dopamine innervation and neuronal activity of globus pallidus. Neuroscience, 2009. 164(2): p. 588-96.

57. Chan, C.S., et al., HCN channelopathy in external globus pallidus neurons in models of Parkinson's disease. Nat Neurosci, 2011. 14(1): p. 85-92.

58. Ruskin, D.N., et al., Multisecond oscillations in firing rate in the basal ganglia: robust modulation by dopamine receptor activation and anesthesia. J Neurophysiol, 1999. 81(5): p. 2046-55.

59. Lee, C.R., E.D. Abercrombie, and J.M. Tepper, Pallidal control of substantia nigra dopaminergic neuron firing pattern and its relation to extracellular neostriatal dopamine levels. Neuroscience, 2004. 129(2): p. 481-9.

60. Bateup, H.S., et al., Distinct subclasses of medium spiny neurons differentially regulate striatal motor behaviors. Proc Natl Acad Sci U S A, 2010. 107(33): p. 14845-50.

61. Tepper, J.M. and C.R. Lee, GABAergic control of substantia nigra dopaminergic neurons. Prog Brain Res, 2007. 160: p. 189-208.

62. Lee, C.S., H. Sauer, and A. Bjorklund, Dopaminergic neuronal degeneration and motor impairments following axon terminal lesion by instrastriatal 6-hydroxydopamine in the rat. Neuroscience, 1996. 72(3): p. 641-53.

63. Gasca-Martinez, D., et al., Dopamine inhibits GABA transmission from the globus pallidus to the thalamic reticular nucleus via presynaptic D4 receptors. Neuroscience, 2010. 169(4): p. 1672-81.

64. Kita, H. and T. Kita, Cortical stimulation evokes abnormal responses in the dopamine-depleted rat basal ganglia. J Neurosci, 2011. 31(28): p. 10311-22.

65. Bevan, M.D., et al., Move to the rhythm: oscillations in the subthalamic nucleus-external globus pallidus network. Trends Neurosci, 2002. 25(10): p. 525-31.

66. Bevan, M.D., et al., Selective innervation of neostriatal interneurons by a subclass of neuron in the globus pallidus of the rat. J Neurosci, 1998. 18(22): p. 9438-52.

67. Magill, P.J., J.P. Bolam, and M.D. Bevan, Dopamine regulates the impact of the cerebral cortex on the subthalamic nucleus-globus pallidus network. Neuroscience, 2001. 106(2): p. 313-30.

68. Magill, P.J., et al., Brain state-dependency of coherent oscillatory activity in the cerebral cortex and basal ganglia of the rat. J Neurophysiol, 2004. 92(4): p. 2122-36.

69. Zold, C.L., et al., Nigrostriatal lesion induces D2-modulated phase-locked activity in the basal ganglia of rats. Eur J Neurosci, 2007. 25(7): p. 2131-44.

70. Mallet, N., et al., Parkinsonian beta oscillations in the external globus pallidus and their relationship with subthalamic nucleus activity. J Neurosci, 2008. 28(52): p. 14245-58.

71. Hutchinson, W.D., et al., Effects of apomorphine on globus pallidus neurons in parkinsonian patients. Ann Neurol, 1997. 42(5): p. 767-75.

72. Stefani, A., et al., Electrophysiological and clinical desensitization to apomorphine administration in parkinsonian patients undergoing stereotaxic neurosurgery. Exp Neurol, 1999. 156(1): p. 209-13.

73. Levy, R., et al., Effects of apomorphine on subthalamic nucleus and globus pallidus internus neurons in patients with Parkinson's disease. J Neurophysiol, 2001. 86(1): p. 249-60.

74. Williams, D., et al., Dopamine-dependent changes in the functional connectivity between basal ganglia and cerebral cortex in humans. Brain, 2002. 125(Pt 7): p. 1558-69.

75. Nishibayashi, H., et al., Cortically evoked responses of human pallidal neurons recorded during stereotactic neurosurgery. Mov Disord, 2011. 26(3): p. 469-76.

76. Raz, A., E. Vaadia, and H. Bergman, Firing patterns and correlations of spontaneous discharge of pallidal neurons in the normal and the tremulous 1-methyl-4-phenyl-1,2,3,6-tetrahydropyridine vervet model of parkinsonism. J Neurosci, 2000. 20(22): p. 8559-71.

77. Bugaysen, J., et al., Electrophysiological characteristics of globus pallidus neurons. PLoS One, 2010. 5(8): p. e12001.

78. Benhamou, L., et al., Globus Pallidus external segment neuron classification in freely moving rats: a comparison to primates. PLoS One, 2012. 7(9): p. e45421.

79. Miguelez, C., et al., Altered pallido-pallidal synaptic transmission leads to aberrant firing of globus pallidus neurons in a rat model of Parkinson's disease. J Physiol, 2012. 590(Pt 22): p. 5861-75.

80. Filion, M., Effects of interruption of the nigrostriatal pathway and of dopaminergic agents on the spontaneous activity of globus pallidus neurons in the awake monkey. Brain Res, 1979. 178(2-3): p. 425-41.

81. Filion, M. and L. Tremblay, Abnormal spontaneous activity of globus pallidus neurons in monkeys with MPTP-induced parkinsonism. Brain Res, 1991. 547(1): p. 142-51.

82. Filion, M., L. Tremblay, and P.J. Bedard, Effects of dopamine agonists on the spontaneous activity of globus pallidus neurons in monkeys with MPTP-induced parkinsonism. Brain Res, 1991. 547(1): p. 152-61.

83. Nini, A., et al., Neurons in the globus pallidus do not show correlated activity in the normal monkey, but phase-locked oscillations appear in the MPTP model of parkinsonism. J Neurophysiol, 1995. 74(4): p. 1800-5.

84. Boraud, T., et al., Effects of L-DOPA on neuronal activity of the globus pallidus externalis (GPe) and globus pallidus internalis (GPi) in the MPTP-treated monkey. Brain Res, 1998. 787(1): p. 157-60.

85. Goldberg, J.A., et al., Enhanced synchrony among primary motor cortex neurons in the 1-methyl-4-phenyl-1,2,3,6-tetrahydropyridine primate model of Parkinson's disease. J Neurosci, 2002. 22(11): p. 4639-53.

86. Heimer, G., et al., Dopamine replacement therapy reverses abnormal synchronization of pallidal neurons in the 1-methyl-4-phenyl-1,2,3,6-tetrahydropyridine primate model of parkinsonism. J Neurosci, 2002. 22(18): p. 7850-5.

87. Wichmann, T., M.A. Kliem, and J. Soares, Slow oscillatory discharge in the primate basal ganglia. J Neurophysiol, 2002. 87(2): p. 1145-8.

88. Hong, S. and O. Hikosaka, The globus pallidus sends reward-related signals to the lateral habenula. Neuron, 2008. 60(4): p. 720-9.

89. Soares, J., et al., Role of external pallidal segment in primate parkinsonism: comparison of the effects of 1-methyl-4-phenyl-1,2,3,6-tetrahydropyridine-induced parkinsonism and lesions of the external pallidal segment. J Neurosci, 2004. 24(29): p. 6417-26.

90. Meredith, G.E. and U.J. Kang, Behavioral models of Parkinson's disease in rodents: a new look at an old problem. Mov Disord, 2006. 21(10): p. 1595-606.

91. Schallert, T. and M.D. Lindner, Rescuing neurons from trans-synaptic degeneration after brain damage: helpful, harmful, or neutral in recovery of function? Can J Psychol, 1990. 44(2): p. 276-92.

92. Schaar, K.L., M.M. Brenneman, and S.I. Savitz, Functional assessments in the rodent stroke model. Exp Transl Stroke Med, 2010. 2(1): p. 13.

93. Buck, K., P. Voehringer, and B. Ferger, Site-specific action of L-3,4-dihydroxyphenylalanine in the striatum but not globus pallidus and substantia nigra pars reticulata evokes dyskinetic movements in chronic L-3,4-dihydroxyphenylalanine-treated 6-hydroxydopamine-lesioned rats. Neuroscience, 2010. 166(2): p. 355-8.

94. Xu, D., et al., Effects of L-DOPA on nigral dopamine neurons and local field potential: comparison with apomorphine and muscimol. J Pharmacol Exp Ther, 2011. 337(2): p. 533-9.

95. Guyenet, P.G. and G.K. Aghajanian, Antidromic identification of dopaminergic and other output neurons of the rat substantia nigra. Brain Res, 1978. 150(1): p. 69-84.

96. Shi, W.X., C.L. Pun, and Y. Zhou, Psychostimulants induce low-frequency oscillations in the firing activity of dopamine neurons. Neuropsychopharmacology, 2004. 29(12): p. 2160-7.

97. Shi, W.X., Slow oscillatory firing: a major firing pattern of dopamine neurons in the ventral tegmental area. J Neurophysiol, 2005. 94(5): p. 3516-22.

98. Gao, M., et al., Functional coupling between the prefrontal cortex and dopamine neurons in the ventral tegmental area. J Neurosci, 2007. 27(20): p. 5414-21.

99. Godfraind, J.M., [Localization of glass microelectrode extremities in the central nervous system by pontamine electrophoresis]. J Physiol (Paris), 1969. 61 Suppl 2: p. 436-7.

100. Hellon, R.F., The marking of electrode tip positions in nervous tissue. J Physiol, 1971. 214 Suppl: p. 12P.

101. Holt, G.R., et al., Comparison of discharge variability in vitro and in vivo in cat visual cortex neurons. J Neurophysiol, 1996. 75(5): p. 1806-14.

102. Slezia, A., et al., Phase advancement and nucleus-specific timing of thalamocortical activity during slow cortical oscillation. J Neurosci, 2011. 31(2): p. 607-17.

103. Nisenbaum, E.S., W.B. Orr, and T.W. Berger, Evidence for two functionally distinct subpopulations of neurons within the rat striatum. J Neurosci, 1988. 8(11): p. 4138-50.

104. Bevan, M.D., C.M. Francis, and J.P. Bolam, The glutamate-enriched cortical and thalamic input to neurons in the subthalamic nucleus of the rat: convergence with GABA-positive terminals. J Comp Neurol, 1995. 361(3): p. 491-511.

105. Kita, T. and H. Kita, The subthalamic nucleus is one of multiple innervation sites for long-range corticofugal axons: a single-axon tracing study in the rat. J Neurosci, 2012. 32(17): p. 5990-9.

106. Crunelli, V. and S.W. Hughes, The slow (<1 Hz) rhythm of non-REM sleep: a dialogue between three cardinal oscillators. Nat Neurosci, 2010. 13(1): p. 9-17.

107. Castle, M., et al., Thalamic innervation of the direct and indirect basal ganglia pathways in the rat: Ipsi- and contralateral projections. J Comp Neurol, 2005. 483(2): p. 143-53.

108. Lanciego, J.L., et al., Thalamic innervation of striatal and subthalamic neurons projecting to the rat entopeduncular nucleus. Eur J Neurosci, 2004. 19(5): p. 1267-77.

109. Pienaar, I.S., B. Lu, and T. Schallert, Closing the gap between clinic and cage: sensori-motor and cognitive behavioural testing regimens in neurotoxin-induced animal models of Parkinson's disease. Neurosci Biobehav Rev, 2012. 36(10): p. 2305-24.

110. Lundblad, M., et al., Pharmacological validation of behavioural measures of akinesia and dyskinesia in a rat model of Parkinson's disease. Eur J Neurosci, 2002. 15(1): p. 120-32.

111. Kirik, D., et al., Long-term rAAV-mediated gene transfer of GDNF in the rat Parkinson's model: intrastriatal but not intranigral transduction promotes functional regeneration in the lesioned nigrostriatal system. J Neurosci, 2000. 20(12): p. 4686-700.

112. Kirik, D., C. Rosenblad, and A. Bjorklund, Characterization of behavioral and neurodegenerative changes following partial lesions of the nigrostriatal dopamine system induced by intrastriatal 6-hydroxydopamine in the rat. Exp Neurol, 1998. 152(2): p. 259-77.

113. Schallert, T., et al., CNS plasticity and assessment of forelimb sensorimotor outcome in unilateral rat models of stroke, cortical ablation, parkinsonism and spinal cord injury. Neuropharmacology, 2000. 39(5): p. 777-87.

114. Iancu, R., et al., Behavioral characterization of a unilateral 6-OHDA-lesion model of Parkinson's disease in mice. Behav Brain Res, 2005. 162(1): p. 1-10.